Supporting information

Net-clipping as a top-down approach for the prediction of topologies of MOFs built from reduced-symmetry linkers

Borja Ortín-Rubio,[a,b] Jaume Rostoll-Berenguer,[c] Carlos Vila,[c] Davide M. Proserpio,[d] Vincent Guillerm,[e] Judith Juanhuix,[f] Inhar Imaz,*[a] and Daniel Maspoch *[a,b,g]

[a] Catalan Institute of Nanoscience and Nanotechnology (ICN2), CSIC and The Barcelona Institute of Science and Technology, Campus UAB, Bellaterra, 08193 Barcelona, Spain
[b] Departament de Química, Facultat de Ciències, Universitat Autònoma de Barcelona, 08193 Bellaterra, Spain
[c] Departament de Química Orgànica, Facultat de Química, Universitat de València, 46100 Burjassot, València, Spain
[d] Dipartamento di Chimica, Università degli Studi di Milano, Milano, 20133, Italy
[e] Division of Physical Sciences and Engineering, Advanced Membranes & Porous Materials Center (AMPM), Functional Materials Design, Discovery & Development Research Group (FMD3), King Abdullah University of Science and Technology (KAUST), Thuwal 23955-6900, Kingdom of Saudi Arabia
[f] ALBA Synchrotron, 08290 Cerdanyola del Vallès, Barcelona, Spain
[g] ICREA, Pg. Lluís Companys 23, 08010 Barcelona, Spain

Table of contents

S1. Materials, methods and characterization

S1.1. Materials

Copper(II) nitrate hemi(pentahydrate) ($Cu(NO_3)_2·2.5H_2O$), potassium carbonate (K_2CO_3), potassium iodide (KI), sodium hydroxide (NaOH), *n*-butyllithium solution (*n*-BuLi), *N,N,N',N'*-tetramethylethylenediamine (TMEDA), paraformaldehyde, *tert*-butanol (*t*-BuOH), Celite® 512 medium, 2,4-dimethoxybenzene and magnesium sulfate (Mg_2SO_4) were purchased from Sigma-Aldrich Co. *N,N*-dimethylformamide (DMF), acetone, tetrahydrofuran (THF), hexane, ethylacetate (AcOEt), methanol (MeOH), hydrochloric acid (HCl), dichloromethane (DCM) and diethyl ether (Et_2O) were obtained from Fisher Chemical. Potassium permanganate ($KMnO_4$) and anhydrous sodium sulfate were obtained from Panreac AppliChem. Anhydrous iron chloride ($FeCl_3$) was purchased from Acros Organics. Sodium borohydride ($NaBH_4$) was obtained from Thermo Scientific Chemicals. 2,4-Dimethoxy-1-methylbenzene, methyl 3-hydroxybenzoate and 1,2,4,5-tetrakis(bromomethyl)benzene were purchased from BLDpharm. All the reagents and solvents were used without further purification unless otherwise specified. Deionized water was obtained with a Milli-Q® system (18.2 MΩ·cm).

S1.2. Methods

Generation and discovery of derived nets

For the generation of the derived nets, we used Materials Studio 2021 Program and the following procedure:

(i)   We first imposed a less-symmetric group related to the one of the main topology by translation-equivalent and class-equivalent subgroup according to the International Tables of Crystallography.[1]

(ii)   We created mass centroids in the middle point between the atom splitted and two neighbouring atoms.

(iii)   We substituted the clippable node by a set of less-symmetric nodes and edges by inserting atoms in the coordinates of the mass centroids.

(iv)   And we repeated this process with a different set of atoms, splitting the node in the different possible directions.

The resulting 102 underlying nets were analysed with the ToposPro 5. 5. 1. 0 program and the TopCryst website (https://topcryst.com/).

Net-clipping

Net-clipping approach was performed by using Materials Studio 2021 Program. Removing symmetrically half of the nodes (and their connections) was carried out by different methods depending on the space group related to each net. Generally, the adjacent nodes to the clippable node are related by symmetry in the derived nets. Accordingly, it was necessary to break this symmetry by (i) imposing *P1* symmetry, or (ii) creating a supercell of different dimensions (depending on the net) to find the smallest repeating unit, in which these nodes can be removed independently. Then, we removed half of the selected nodes to generate less-symmetric nodes (Figure 1). Each of the 102 derived nets were clipped using these two methods. The resulting 46 underlying nets were analysed with the ToposPro 5. 5. 1. 0 program and the TopCryst website (https://topcryst.com/).

S1.3. Synthesis

Synthesis of 3,3',3'',3'''-[1,2,4,5-phenyltetramethoxy]tetrabenzoic acid (H₄PTMTB)
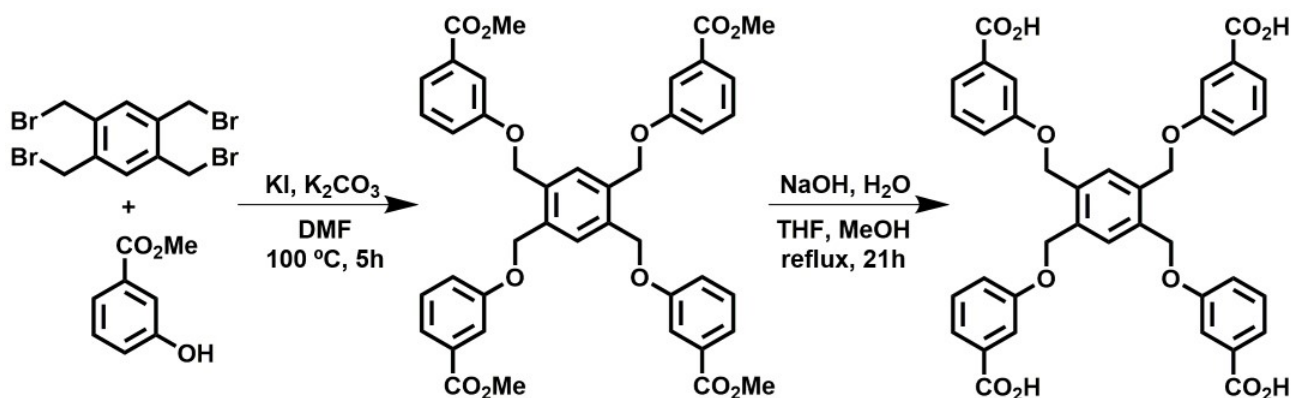
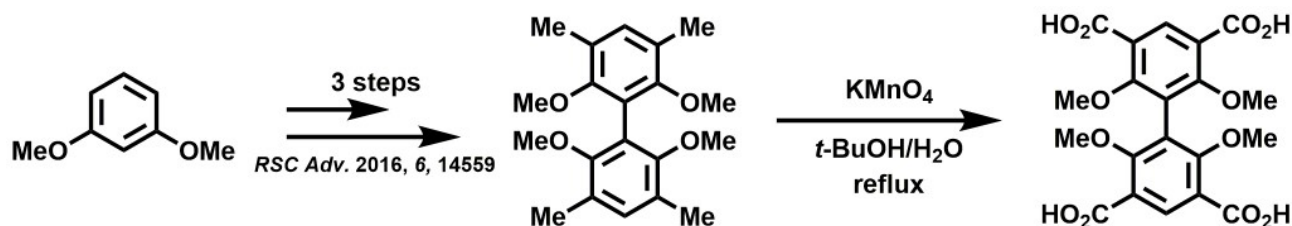**Scheme S1.** Synthetic procedure for H₄PTMTB linker.

Synthesis of tetramethyl 3,3',3'',3'''-[1,2,4,5-phenyltetramethoxy]tetrabenzoate

This compound was synthesized according to a similar literature procedure.[2] Methyl 3-hydroxybenzoate (1.15 g, 7.55 mmol) was dissolved in DMF (40 mL) under Ar atmosphere. KI (38.7 mg, 0.23 mmol) and K_2CO_3 (2.19 g, 15.88 mmol) were added to the solution. The solution was heated to 100 ºC for 1 h. Then, a solution of 1,2,4,5-tetrakis(bromomethyl)benzene (0.66 g, 1.47 mmol) in DMF (15 mL) was added dropwise. The reaction was heated at 100 ºC during 5 h, and then cooled to room temperature. After the addition of H_2O (350 mL) to the solution, a precipitate was formed, which was filtered, washed with H_2O and dried at 65 ºC. The solid was heated to reflux overnight in MeOH (150 mL). Finally, it was filtered in hot, washed with MeOH and dried at 65 ºC to afford a white solid (0.86 g, 79 %). **¹H NMR (300 MHz, CDCl₃) δ** 7.72 (s, 2H), 7.67 (d, J = 7.6 Hz, 8H), 7.35 (t, J = 7.9 Hz, 4H), 7.16 (m, 4H), 5.26 (s, 8H), 3.92 (s, 12H); **¹³C NMR (75 MHz, CDCl₃) δ** 166.8 (C), 158.4 (C), 135.2 (C), 131.6 (CH), 129.9 (CH),129.6 (CH), 122.6 (C), 120.0 (CH), 115.1 (CH), 67.8 (CH₂), 52.2 (CH₃).

Synthesis of 3,3',3'',3'''-[1,2,4,5-phenyltetramethoxy]tetrabenzoic acid (H₄PTMTB)

Tetramethyl 3,3',3'',3'''-[1,2,4,5-phenyltetramethoxy]tetrabenzoate was suspended in a THF (200 mL) and MeOH (20 mL) mixture. An aqueous solution of NaOH (1.6 g, 40 mmol; 100 mL) was added and the reaction was heated at 90 ºC for 21 h. It was then concentrated under reduced pressure, diluted with H_2O (100 mL) and washed with AcOEt (70 mL, discarded). Then, a 2N HCl solution was added dropwise to pH = 1, producing a white solid precipitate. The solid was filtered, washed with H_2O and dried at 65 ºC to afford a white solid (0.61 g, 60 %). **¹H NMR (300 MHz, DMSO) δ** 12.97 (s, 4H), 7.75 (s, 2H), 7.54 (d, J = 8.3 Hz, 8H), 7.40 (t, J = 7.8 Hz, 4H), 7.27 (d, J = 6.9 Hz, 4H), 5.33 (s, 8H); **¹³C NMR (75 MHz, CDCl₃) δ** 167.5 (C), 158.7 (C), 139.3 (C), 135.3 (CH), 132.7 (CH),130.2 (CH), 122.4 (C), 120.1 (CH), 115.5 (CH), 67.4 (CH₂).

Synthesis of 2,2',6,6'-tetramethoxy-[1,1'-biphenyl]-3,3',5,5'-tetracarboxylic acid (H₄TMBPTC)

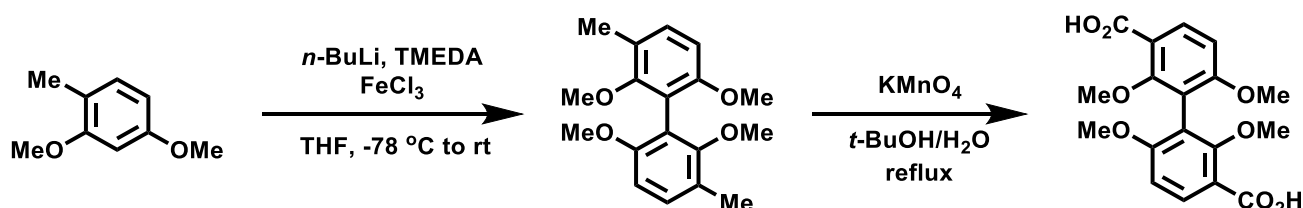**Scheme S2.** Synthetic procedure for H₄TMBPTC linker.

Synthesis of 2,2',6,6'-tetramethoxy-3,3',5,5'-tetramethyl-1,1'-biphenyl

2,2',6,6'-tetramethoxy-3,3'-dimethyl-1,1'-biphenyl was synthesized according to a previous reported procedure.[3]

Synthesis of 2,2',6,6'-tetramethoxy-[1,1'-biphenyl]-3,3',5,5'-tetracarboxylic acid (H₄TMBPTC)

In a 50 mL round bottomed flask, 2,2',6,6'-tetramethoxy-3,3',5,5'-tetramethyl-1,1'-biphenyl (451.7 mg, 1.37 mmol, 1 equiv.) was placed and dissolved in a mixture of t-BuOH:H_2O 1:1 (10+10 mL). Then, $KMnO_4$ (4.6 g, 29 mmol, 10 equiv.) was added and the solution was heated to reflux until the characteristic purple colour of $KMnO_4$ faded (approximately 7 h). The suspension was thereafter filtered over Celite, rinsed with the minimum amount of water, and concentrated under reduced pressure to dryness. HCl 2 M was added until acidic pH (<3) and it was concentrated again to dryness. Then, the white solid was dispersed in acetone, also adding anhydrous Na_2SO_4 to remove traces of water. The solution was filtered and concentrated under reduced pressure. Finally, the residue was purified by flash column chromatography using DCM:acetone mixtures (from 90:10 to 50:50) to afford 2,2',6,6'-tetramethoxy-[1,1'-biphenyl]-3,3',5,5'-tetracarboxylic acid (620.7 mg, 1.71 mmol, 59% yield). **¹H NMR (300 MHz, DMSO-d_6) δ** 8.24 (s, 2H), 3.59 (s, 12H); **¹³C NMR (75 MHz, DMSO-d_6) δ** 166.1 (C), 161.3 (C), 134.8 (CH), 123.5 (C), 119.7 (C), 61.7 (CH₃).

Synthesis of 2,2',6,6'-tetramethoxy-[1,1'-biphenyl]-3,3'-dicarboxylic acid (H₂TMBPDC)

Scheme S3. Synthetic procedure for H₂TMBPDC linker.

Synthesis of 2,2',6,6'-tetramethoxy-3,3'-dimethyl-1,1'-biphenyl

2,4-Dimethoxy-1-methylbenzene (913 mg, 6 mmol, 1 equiv.) was weighted in an oven-dried Schlenk flask and it was subjected to vacuum/N_2 cycles (x3). Then, freshly distilled THF (10 mL) and dry TMEDA (1.08 mL, 7.2 mmol, 1.2 equiv.) were successively introduced via syringe. Thereafter, the solution was cooled down to -78 °C and it was stirred at that temperature for 5 min. After this period, n-BuLi (4.2 mL, 1.6 M in THF, 6.6 mmol, 1.1 equiv.) was slowly added using a programmable pump (8.4 mL/h). Once the addition was completed, the resulting mixture was stirred 10 min at -78 °C and then, the bath was removed, allowing the solution to reach room

temperature. After stirring the solution for 3 h at room temperature, a solution of anhydrous $FeCl_3$ (1.17 g, 7.2 mmol, 1.2 equiv.) in dry THF (10 mL) under N_2 was added via cannula, causing the solution to change from light yellow to dark red. This solution was further stirred for 16 h and then, quenched by the dropwise addition of HCl 10% (10 mL). Et_2O (30 mL) was also added, and the phases were separated. The aqueous phase was further extracted with Et_2O (2x20 mL) and the combined organic phases were dried over anhydrous $MgSO_4$, filtered and concentrated under reduced pressure. The oily residue was purified by flash column chromatography using hexane:EtOAc mixtures (from 95:5 to 90:10) as eluent, obtaining 2,2',6,6'-tetramethoxy-3,3'-dimethyl-1,1'-biphenyl (453.6 mg, 1.5 mmol, 50% yield). **^{1}H NMR (300 MHz, CDCl$_3$) δ** 7.15 (dq, J = 8.4, 0.7 Hz, 2H), 6.69 (d, J = 8.4 Hz, 2H), 3.72 (s, 6H), 3.41 (s, 6H), 2.28 (d, J = 0.7 Hz, 6H); **^{13}C NMR (75 MHz, CDCl$_3$) δ** 157.2 (C), 156.6 (C), 130.2 (CH), 123.2 (C), 117.8 (C), 106.4 (CH), 59.7 (CH$_3$), 56.0 (CH$_3$), 15.8 (CH$_3$).

Synthesis of 2,2',6,6'-tetramethoxy-[1,1'-biphenyl]-3,3'-dicarboxylic acid (H$_2$TMBPDC)

In a 50 mL round bottomed flask, 2,2',6,6'-tetramethoxy-3,3'-dimethyl-1,1'-biphenyl (876.7 mg, 2.9 mmol, 1 equiv.) was placed and dissolved in a mixture of t-BuOH:H$_2$O 1:1 (10+10 mL). Then, KMnO$_4$ (2.3 g, 14.5 mmol, 5 equiv.) was added and the solution was heated to reflux until the characteristic purple colour of KMnO$_4$ faded (approximately 5 h). The suspension was thereafter filtered over Celite, rinsed with the minimum amount of water, and concentrated under reduced pressure to dryness. HCl 2 M was added until acidic pH (<3) and it was concentrated again to dryness. Then, the white solid was dispersed in acetone, also adding anhydrous Na$_2$SO$_4$ to remove traces of water. The solution was filtered and concentrated under reduced pressure. Finally, the residue was purified by flash column chromatography using DCM:acetone mixtures (from 90:10 to 50:50) to afford 2,2',6,6'-tetramethoxy-[1,1'-biphenyl]-3,3'-dicarboxylic acid (620.7 mg, 1.71 mmol, 59% yield). **^{1}H NMR (500 MHz, DMSO-d_6) δ** 7.83 (d, J = 8.7 Hz, 2H), 6.92 (d, J = 8.8 Hz, 2H), 3.71 (s, 6H), 3.44 (s, 6H); **^{13}C NMR (125 MHz, DMSO-d_6) δ** 166.7 (C), 160.9 (C), 159.1 (C), 132.5 (CH), 117.8 (C), 117.4 (C), 106.4 (CH), 61.1 (CH$_3$), 55.8 (CH$_3$).

Synthesis of Cu$_2$(PTMTB)(H$_2$O)$_2$

Cu(NO$_3$)$_2$·2.5H$_2$O (12 mg, 0.05 mmol) and H$_4$PTMTB (27 mg, 0.04 mmol) in DMF (1 mL) and HBF$_4$ (0.1 mL) was prepared in a 23 mL scintillation vial. Then, the sealed vial was placed into a preheated oven at 85 ºC for 24 h. After this period, blue square-shaped crystals suitable for single-crystal X-ray diffraction (SCXRD) were collected by filtration and washed three times by incubating them with 20 mL of fresh DMF for 12 h.

Synthesis of Cu$_2$(TMBPTC)(H$_2$O)$_2$

Cu(NO$_3$)$_2$·2.5H$_2$O (24 mg, 0.1 mmol) and H$_4$TMBPTC (45 mg, 0.1 mmol) in DMF (1 mL) was prepared in a 23 mL scintillation vial. Then, the sealed vial was placed into a preheated oven at 85 ºC for 24 h. After this period, green needle-shaped crystals suitable for SCXRD were collected by filtration and washed three times by incubating them with 20 mL of fresh DMF for 12 h.

Synthesis of Cu(TMBPDC)(H$_2$O)

Cu(NO$_3$)$_2$·2.5H$_2$O (24 mg, 0.1 mmol) and H$_2$TMBPDC (37 mg, 0.1 mmol) in DMF (1 mL) and H$_2$O (1 mL) was prepared in a 23 mL scintillation vial. Then, the sealed vial was placed into a preheated oven at 85 ºC for 24 h. After this period, green needle-shaped crystals suitable for SCXRD were collected by filtration and washed three times by incubating them with 20 mL of fresh DMF for 12 h.

<u>S1.4. Characterization</u>

Single-Crystal X-Ray Diffraction (SCXRD) data for $Cu_2(PTMTB)(H_2O)_2$, $Cu_2(TMBPTC)(H_2O)_2$, and $Cu_2(TMBPDC)_2(H_2O)_2$ were collected at 100 K at XALOC beamline at ALBA synchrotron (0.82656 Å).[4] Data were indexed, integrated and scaled using the XDS program.[5] Absorption correction was not applied. The structures were solved by direct methods and subsequently refined by correction of F2 against all reflections, using SHELXT2018 within Olex2 package.[6-8] All non-hydrogen atoms were refined with anisotropic thermal parameters by full-matrix least-squares calculations on F2 using the program SHELXL2018.[7] We treated the presence of solvent molecules in the cavities of all structures running solvent mask using Olex2 solvent mask.[8] The hydrogen atoms were calculated in their expected positions with the HFIX instruction of SHELXL2018, and refined as riding atoms with Uiso(H) = 1.5 Ueq(C).

Powder X-Ray Diffraction (PXRD) diagrams were collected on a Panalytical X'pert mpd diffractometer with monochromatic Cu-Kα radiation (λ_{Cu} = 1.5406 Å).

Proton Nuclear Magnetic Resonance (¹H NMR) spectra were acquired in Bruker Avance NEO of 300 MHz NMR spectrometer at "Servei de Ressonància Magnètica Nuclear" from Autonomous University of Barcelona (UAB), and in Bruker Avance NEO of 300 MHz, 500 MHz NMR spectrometers at "Servei Central de Suport a la Investigació Experimental (SCIE)" from University of València (UV).

Carbon Nuclear Magnetic Resonance (¹³C NMR) spectra were acquired in Bruker Avance NEO of 300 MHz, 500 MHz NMR spectrometers at "Servei Central de Suport a la Investigació Experimental (SCIE)" from University of València (UV).

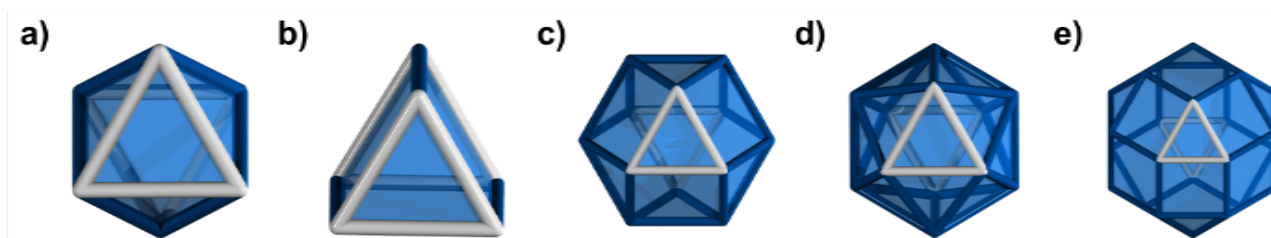## S2. Net-clipping analysis

Figure S1. Schematic of the different MBBs that frustate net-clipping in a symmetrical fashion due to the presence of two triangular faces in the same direction highlighted in a) octahedron, b) triangular prism, c) cuboctahedron, d) icosahedron and e) rhombicuboctahedron.
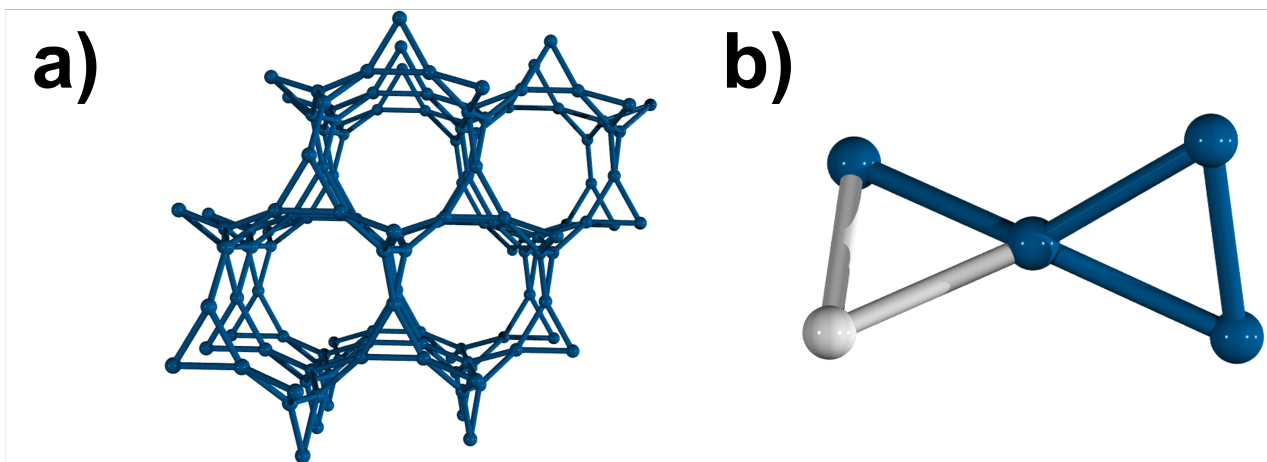
Figure S2. a) **lcv** net and b) highlight of 3-cycles present in this net, which illustrates the frustration of generating a binodal net and therefore, net-clipping.
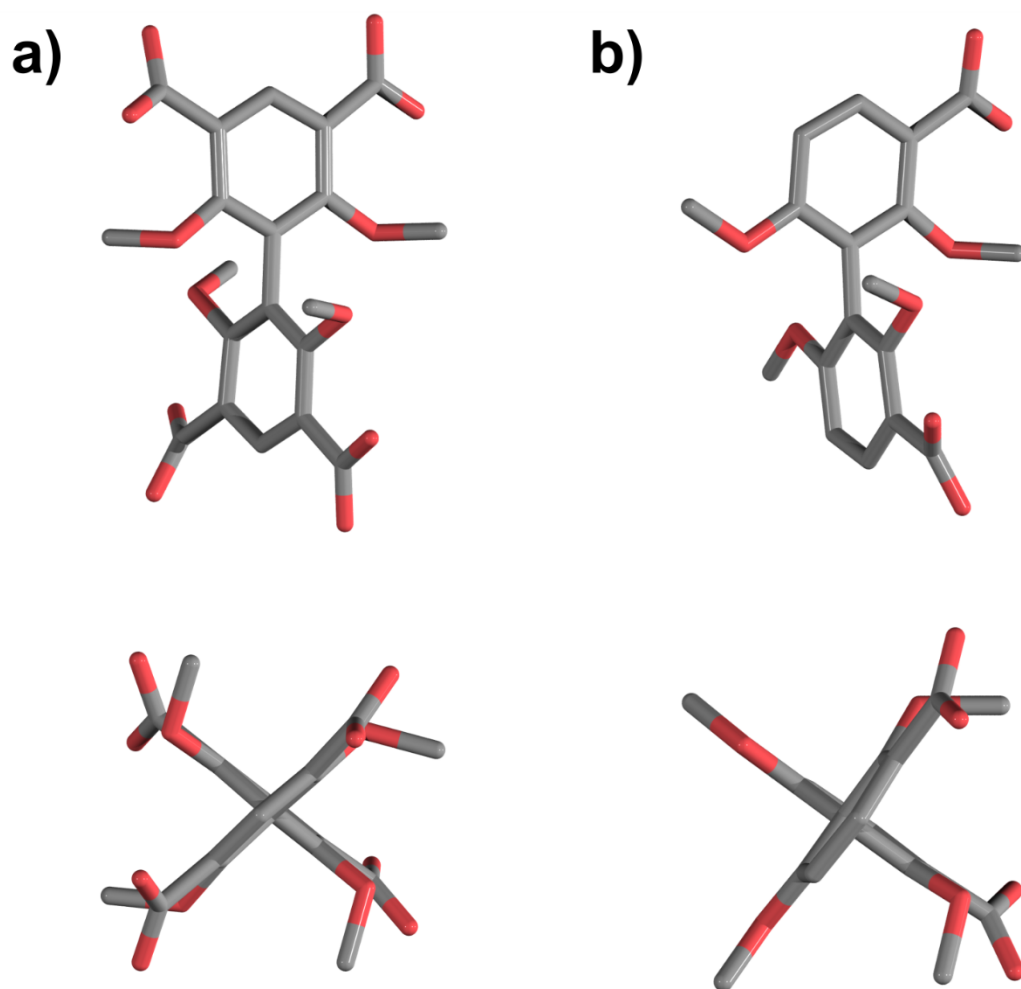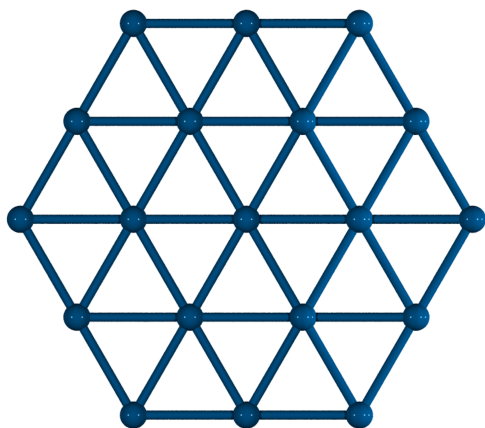
Figure S3. a) TMBPTC and b) TMBPDC linkers showing the steric hindrance of the methoxy groups in the *ortho* positions of the biphenyl MBB that produce the deviation of the carboxylates in 90º respect the others.
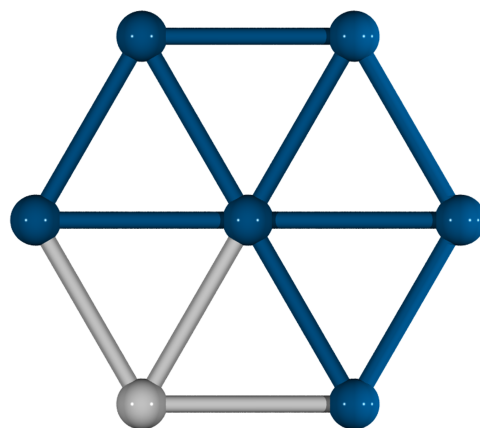
Figure S4. a) **hxl** net and b) highlight of 3-cycle present in this net, which illustrates the frustration of generating a binodal net and therefore, net-clipping.
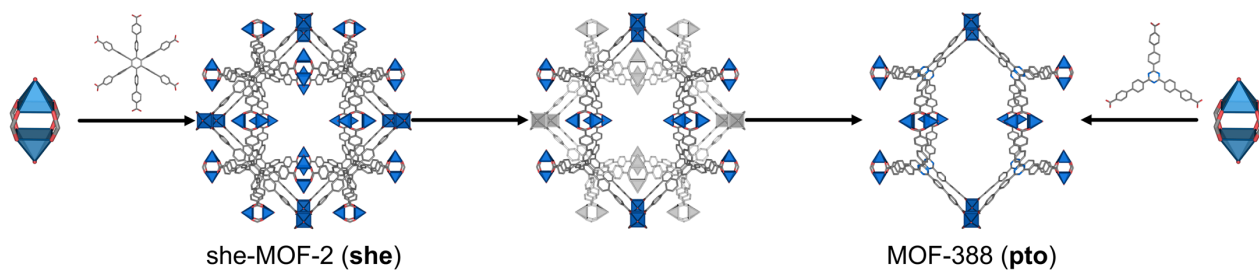
she-MOF-2 (**she**)   MOF-388 (**pto**)

Figure S5. Schematic of the net-clipping approach applied to the formation of reticular materials from hexagonal CBPB ligand to trigonal TAPB combined with 4-c paddle-wheel Cu(II) MBBs.
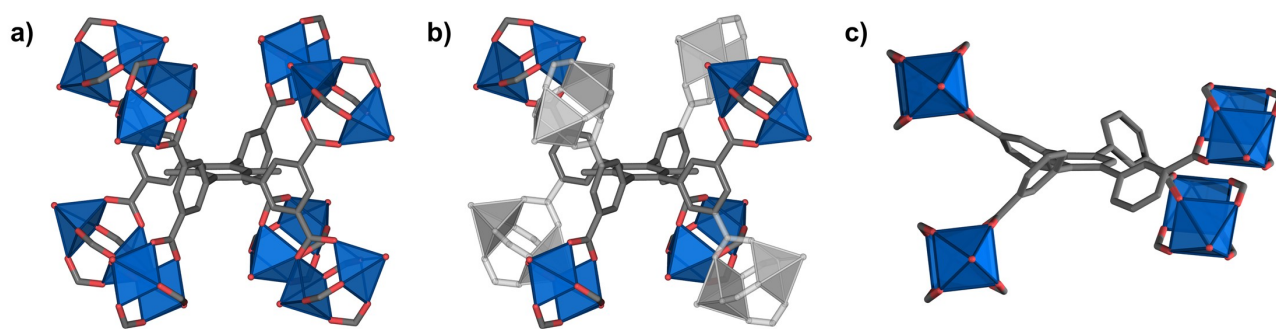
Figure S6. Illustration of a) the conformation of the DMTIB ligand in the crystal structure of ZJNU-10; b) the predicted conformation of the clipped ligand in a square conformation; and c) the conformation of TCPB in the single-crystal structure reticulated with Cu(II)-paddlewheels matching with the prediction made by net-clipping. Note that the approach not only successfully predicted the topology of the MOF assembled with a new low-symmetry linker but also accurately anticipated the conformation adopted by the linker within the structure.

Table S1. Space Group (S.G.), Connectivity (C.), Point Symbol, Transitivity (Trans.), Tiling and D-symbol size for the new derived and clipped *icnx* nets.

Name	S.G.	C.	Point Symbol	Trans.	Tiling	D-symbol
*icn*1	*Pmmm*	4,4,4	$\{4^2.6^2.8^2\}\{4^4.6^2\}_5$	[34]	2-periodic 3D	-
*icn*2	*C222_1*	4,4,4	$\{4.5^2.6.7.8\}\{4.5^3.7.8\}\{5.6.8^4\}$	[3884]	$[4.5^2]+[8^3]+[5^2.6.8^3]$	156
*icn*3	*C222_1*	4,4,4,4	$\{3.4.5.6.7^2\}_2\{3.6.7^2.8^2\}_2\{3^2.4.5^2.6\}\{4.6^2.7.8^2\}$	[4651]	$[3^4.4^2.6^2.7^4.10^2]$	80
*icn*4	*R32*	4,4	$\{4.6^3.8^2\}\{4^3.6^2.8\}$	[2352]	$[4^3.12^2]+[6^3.12^2]$	52
*icn*5	*Pmmm*	3,4,4,4	$\{4.8^2\}_4\{4^2.8^4\}_2\{8^6\}$	[43]	2-periodic 3D	-
*icn*6	*P4_2/mcm*	3,4,4	$\{4.8^2\}_4\{4^2.8^2.10^2\}_2\{8^6\}$	[3243]	$[4^2.8^2]+[4^2.8^2.12^2]+[8^4.12^2]$	32
*icn*7	*I$2_1$3*	3,3,3	$\{10^3\}$	[3334]	$5[10^3]+3[10.12^2]+2[12^3]$	108
*icn*8	*P$6_2$22*	3,4	$\{6^2.10^2.11^2\}\{6^2.10\}_2$	[2232]	$[6.11^2]+[10.11^2]$	60
*icn*9/**lcr**	*I43d*	3,4	$\{8^3\}_2\{8^6\}$	[2221]	$[8^3.9^2]$	28
*icn*10	*R3c*	3,3,4	$\{7^2.8\}\{7^3\}\{7^5.9\}$	[3531]	$[7^{12}.9^2]$	68
*icn*11	*P$6_4$22*	3,4	$\{9^2.10\}_2\{9^4.10^2\}$	[2221]	$[9^4.10^2]$	28
*icn*12	*I$4_1$32*	3,3,4	$\{6^2.10\}_2\{6^2.9^2.10^2\}$	[3344]	$3[6^2.10^2]+2[9^2.10^3]$	64
*icn*13	*Pn3*	3,6	$\{5^3\}_3\{5^6.8^6.10^3\}$	[2222]	$[9^4]+2[5^6.9^2]$	22
*icn*14	*P4_2/nnm*	3,3,6	$\{4.6^2\}_2\{4^2.6^4.8^6.10^3\}\{6^2.8\}$	[3443]	$2[4^2.8^2]+4[6^2.8^2]+[8^4]$	48
*icn*15	*P4_2/nnm*	3,3,6	$\{5.6^2\}_2\{5^2.6\}\{5^4.6^4.8^4.10^2.11\}$	[3432]	$[8^4]+2[5^4.6^2.8^2]$	32
*icn*16	*Ia3*	3,6,6	$\{5^3\}_6\{5^6.8^6.10^3\}\{5^6.8^6.11^3\}$	[3332]	$[10^3]+3[5^2.10^2]$	80
*icn*17	*Ia3d*	3,6	$\{4.9^2\}_3\{4^6.9^6.11^3\}$	[2223]	$2[4^3]+6[4.9^2]+3[9^4]$	44
*icn*18	*I$4_1$32*	3,3,6	$\{6^2.7\}_3\{6^6.7^3.8^6\}$	[3445]	$2[6^3]+3[6.7^2]+3[6.8^2]+3[7^2.8^2]$	84
*icn*19	*I$4_1$32*	3,3,6	$\{4.8^2\}_3\{4^3.6^3.8^3.9^3.10^3\}_2\{6^2.8\}_3$	[3445]	$[4^3]+[6^3]+3[4.9^2]+3[6.8^2]+3[8^2.9^2]$	88
*icn*20	*Ia3*	3,6	$\{6^2.8\}_3\{6^3.8^{12}\}$	[2322]	$[8^6]+[6^6.8^6]$	44
*icn*21	*I$4_1$32*	3,6,6	$\{6^2.7\}_6\{6^3.7^3.8^3.9^6\}\{6^3.7^9.8^3\}$	[33]	self-catenated Hopf link 8-ring	-
*icn*22	*I$2_1$3*	3,3,3,6,6	$\{5.7^2\}_3\{5^2.7\}_3\{5^3.7^3.8^3.9^6\}\{5^3.7^6.8^3.9^3\}$	[5653]	$[8^3]+3[5.7.8^2]+[5^3.7^3.8^3]$	112
*icn*23	*I422*	3,8	$\{5^3\}_4\{5^8.6^4.7^4.8^{12}\}$	[2221]	$[5^8.6^4]$	16
*icn*24	*Pm3n*	3,12	$\{4.6^2\}_6\{4^6.6^{24}.8^{30}.10^6\}$	[2222]	$4[6^3]+3[4^2.6^4]$	14
*icn*25	*P$4_2$32*	3,12	$\{4.6^2\}_6\{4^{12}.6^{18}.8^{30}.10^6\}$	[2233]	$2[4^3]+2[6^3]+3[4^2.6^4]$	26
*icn*26	*Im3m*	3,24	$\{4.6^2\}_{12}\{4^{36}.6^{84}.8^{144}.10^{12}\}$	[2223]	$12[4.6^2]+3[4^4]+4[6^6]$	16
*icn*27	*F4$_1$32*	3,3,12	$\{4.6^2\}_6\{4^{12}.6^{30}.8^{24}\}\{6^3\}_2$	[3223]	$2[4^3]+6[4.6^2]+[6^{12}]$	16
*icn*28	*P432*	3,3,4	$\{8^2.12\}_{12}\{8^3\}_8\{8^4.12^2\}_3$	[32]	self-catenated Multiple link 12-ring	-
*icn*29	*P$6_2$22*	3,3,4,4	$\{6.8^2\}_2\{6.8^4.10\}\{6^2.8^2.10^2\}_2\{6^2.8\}_2$	[44]	self-catenated Hopf link 6-ring	-
*icn*30	*P6/mmm*	3,4,4	$\{4.8^2\}_4\{4^2.6^4\}_2\{8^4.12^2\}$	[3255]	$3[4^2.8^2]+2[4^3.6^2]+2[6^2.8^3]+2[8^6.24^2]$	32
*icn*31	*P6/mmm*	3,4,4	$\{4.8^2\}_4\{4^2.8^2.10^2\}_2\{8^4.12^2\}$	[3255]	$3[4^2.8^2]+4[8^3.12^2]+[4^6.12^2]+[8^6.12^2]$	32
*icn*32	*P62m*	3,3,4,4	$\{4.6^2.8^3\}_2\{4.6^2\}_2\{6.8^2\}_2\{6.8^5\}$	[4465]	$3[4.8^3]+2[6^3.12^2]+2[8^3.12^2]$ $+[4^3.8^3.18^2]+[6^6.18^2]$	68
*icn*33	*P6/m*	3,3,4,4	$\{4.6^2.8^3\}_2\{4.6^2\}_2\{6.8^2\}_2\{6.8^5\}$	[44]	self-catenated Hopf link 8-ring	-
*icn*34	*I422*	3,4,4	$\{8^3\}_4\{8^4.10^2\}\{8^6\}_2$	[32]	self-catenated Hopf link 8-ring	-
*icn*35	*P4/nnc*	3,4,4	$\{8^2.10\}_4\{8^4.10^2\}\{8^6\}_2$	[32]	self-catenated Hopf link 10-ring	-
*icn*36	*I4/mmm*	3,3,4,4,6	$\{4.8^2\}_{12}\{4^6.8^6.10^3\}_4\{8^4.12^2\}\{8^6\}_2$	[5455]	$4[4^3]+8[8^3]+4[4^2.8^2]+2[8^4]+[4^4.8^8]$	60
*icn*37	*Pn3n*	3,4,6	$\{6^2.8^4\}_3\{6^3\}_{12}\{6^6.8^6.10^3\}_4$	[32]	self-catenated Hopf link 6-ring	-
*icn*38	*I432*	3,4,6	$\{4.8^2\}_{12}\{4^3.8^9.10^3\}_4\{8^6\}_3$	[3233]	$12[4.8^2]+12[8^3]+[8^{12}]$	52
*icn*39	*P422*	3,4,8	$\{6^2.8^4\}\{6^3\}_4\{6^8.8^{20}\}$	[32]	self-catenated Hopf link 6-ring	-

S3. Cu$_2$(PTMTB)(H$_2$O)$_2$

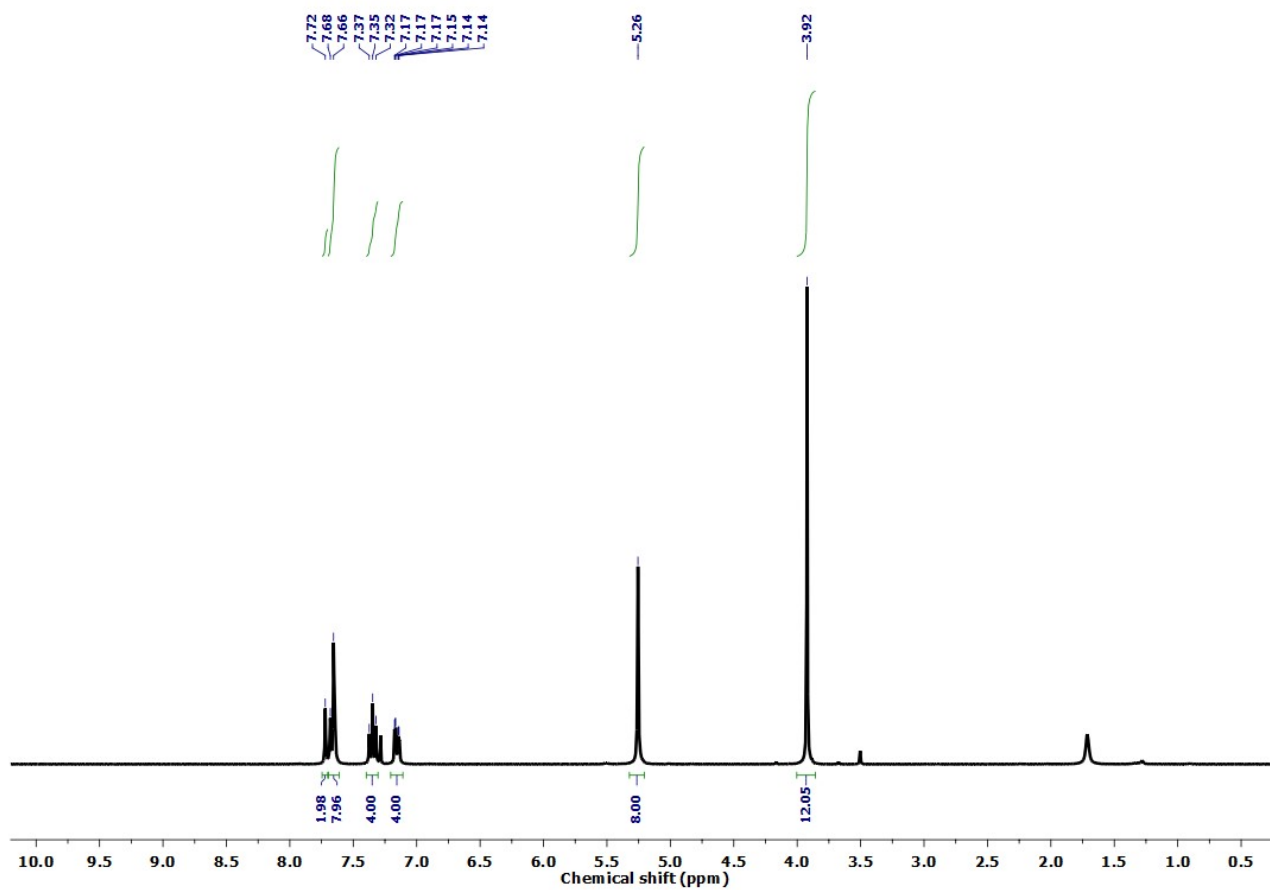### S3.1. ^{1}H and ^{13}C Nuclear Magnetic Resonance

Figure S7. ^{1}H NMR spectrum (300 MHz, CDCl$_3$) of tetramethyl 3,3',3'',3'''-[1,2,4,5-phenyltetramethoxy]tetrabenzoate.
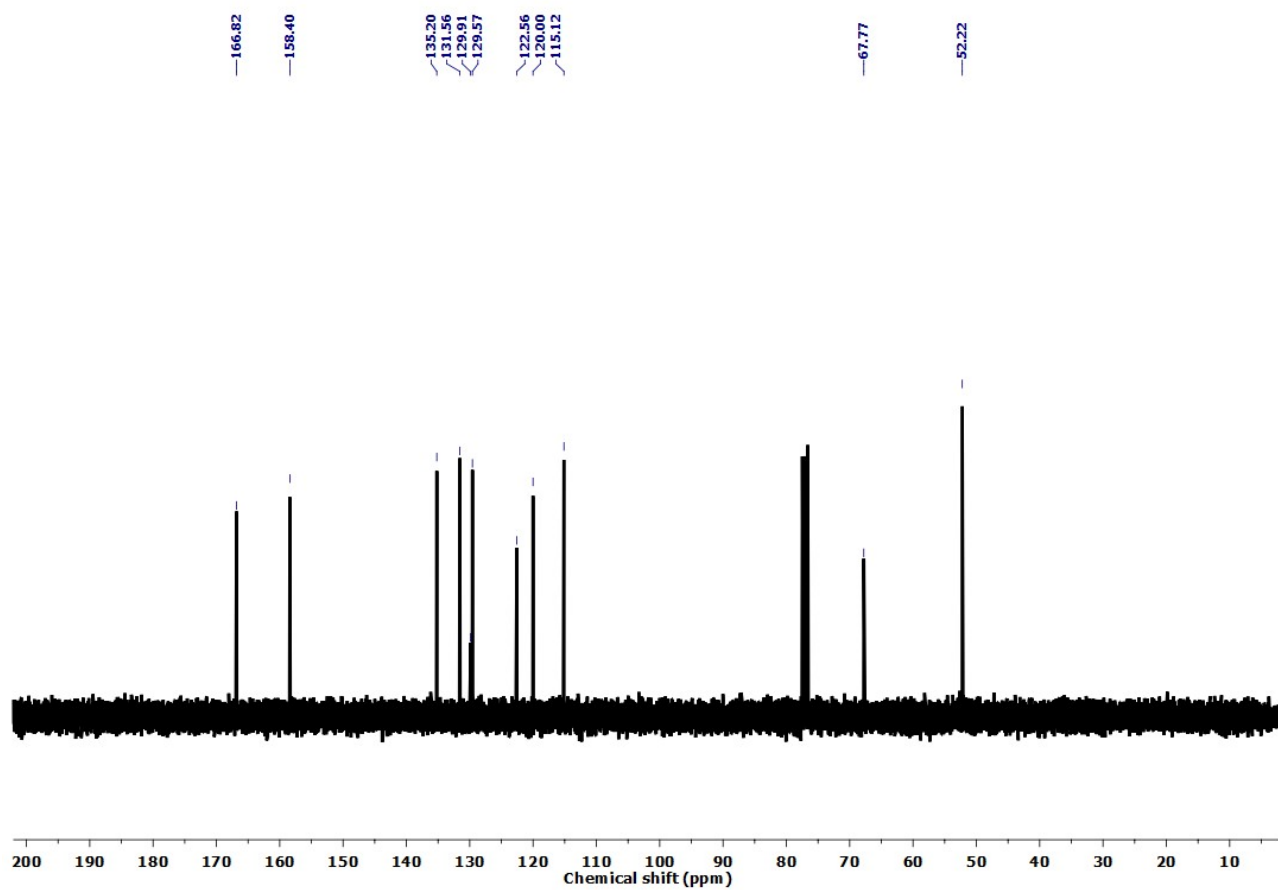
Figure S8. ^{13}C NMR spectrum (75 MHz, CDCl$_3$) of tetramethyl 3,3',3'',3'''-[1,2,4,5-phenyltetramethoxy]tetrabenzoate.
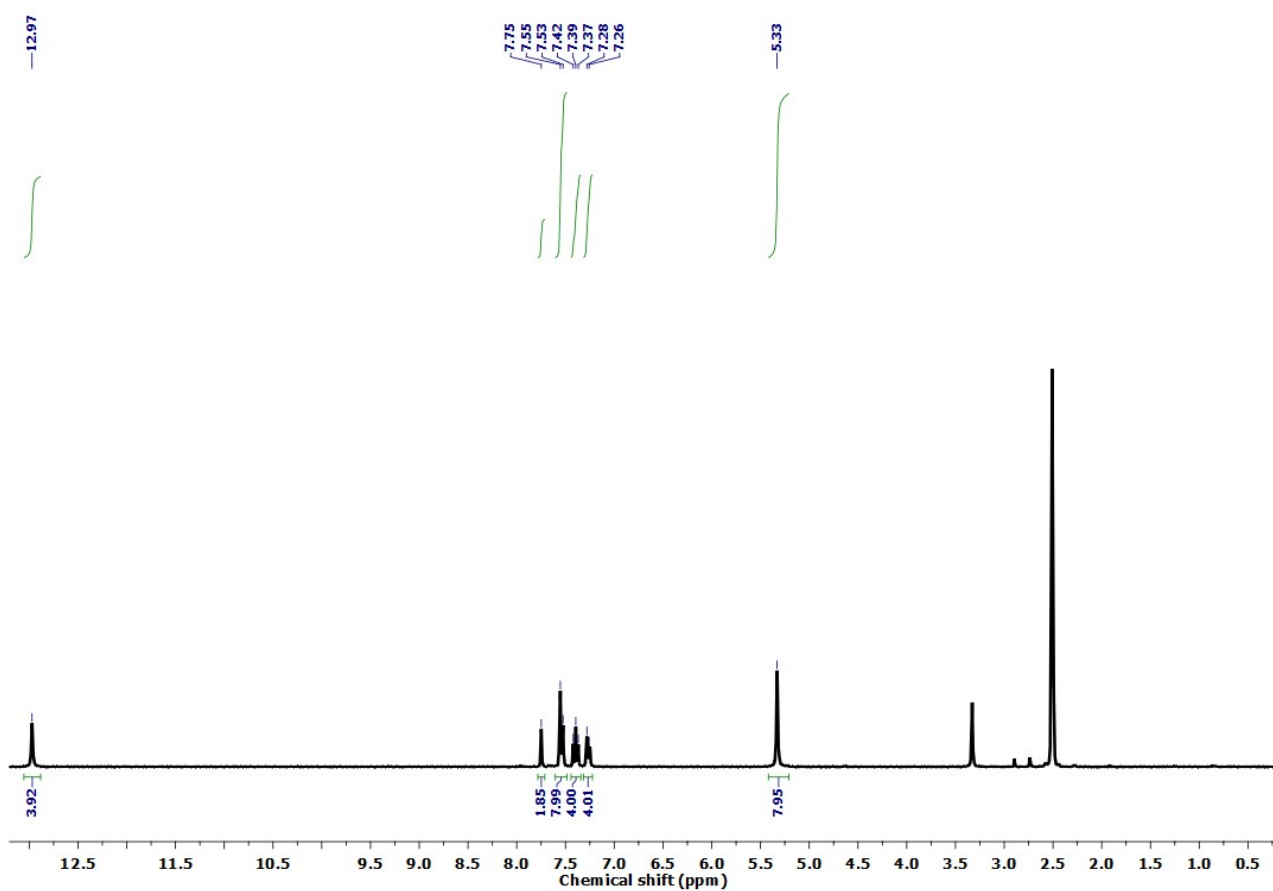
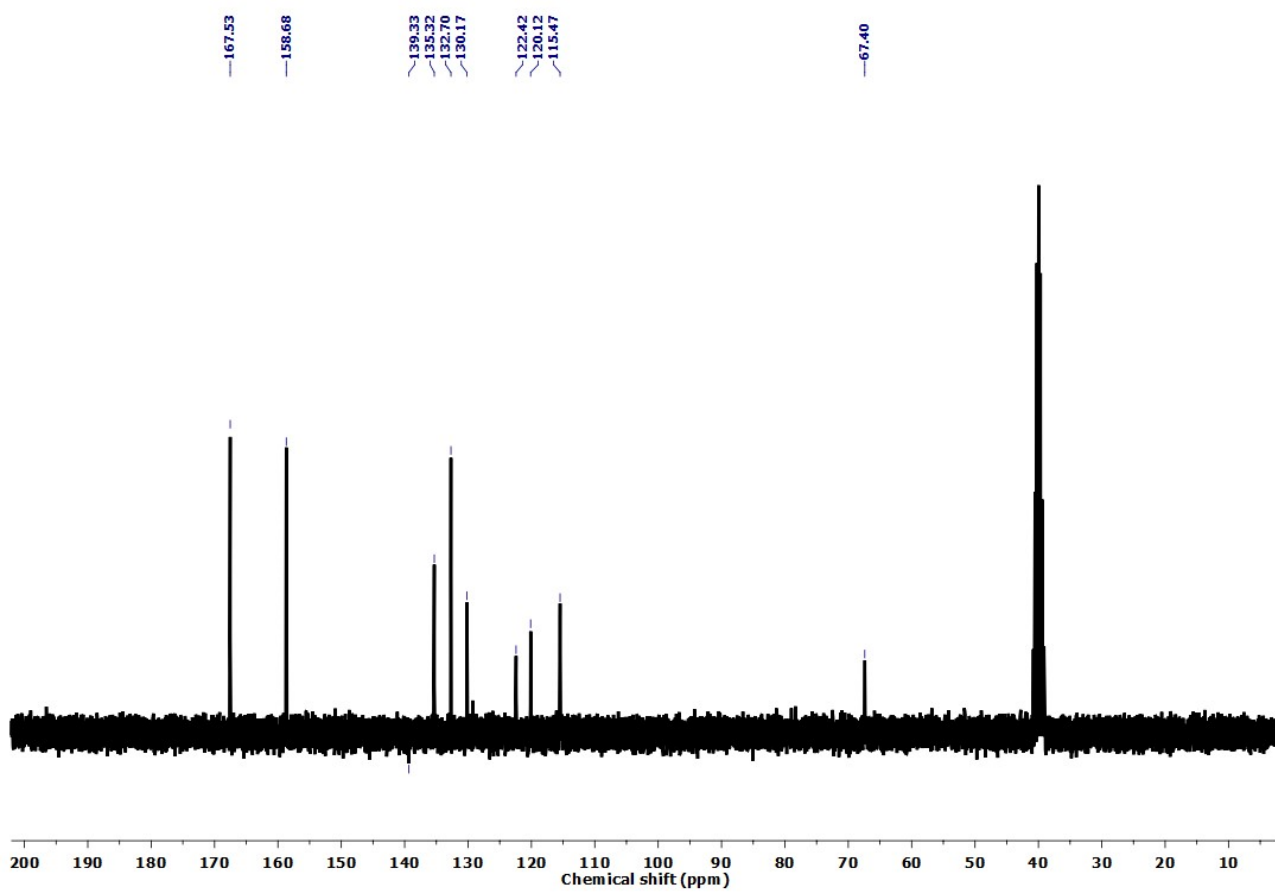**Figure S9.** ^{1}H NMR spectrum (300 MHz, DMSO-d_6) of H$_4$PTMTB.

Figure S10. ^{13}C NMR spectrum (75 MHz, CDCl$_3$) of H$_4$PTMTB.

Peak labels: 167.53, 158.68, 139.33, 135.32, 132.70, 130.17, 122.42, 120.12, 115.47, 67.40

X-axis: Chemical shift (ppm) — 200, 190, 180, 170, 160, 150, 140, 130, 120, 110, 100, 90, 80, 70, 60, 50, 40, 30, 20, 10

S3.2. Single-crystal X-ray diffraction

Table S2. Crystal data and structure refinement for $Cu_2(PTMTB)(H_2O)_2$

Identification code	CCDC-2270219
Empirical formula	$C_{23.38}H_{16}Cu_{1.23}O_{7.38}$
Formula weight	493.33
Temperature/K	100
Crystal system	orthorhombic
Space group	Cmce
a/Å	32.415(3)
b/Å	23.5559(3)
c/Å	16.0326(2)
α/°	90
β/°	90
γ/°	90
Volume/Å^3	12241.8(13)
Z	13
$\rho_{calc}g/cm^3$	0.870
μ/mm^{-1}	1.101
F(000)	3264.0
Crystal size/mm^3	0.11 × 0.1 × 0.08
Radiation	synchrotron (λ = 0.82653)
2Θ range for data collection/°	3.86 to 67.616
Index ranges	0 ≤ h ≤ 43, 0 ≤ k ≤ 29, -20 ≤ l ≤ 0
Reflections collected	73235
Independent reflections	7164 [R_{int} = 0.1582, R_{sigma} = 0.1028]
Data/restraints/parameters	7164/10/226
Goodness-of-fit on F^2	1.065
Final R indexes [I>=2σ (I)]	R_1 = 0.1077, wR_2 = 0.2922
Final R indexes [all data]	R_1 = 0.1156, wR_2 = 0.2957
Largest diff. peak/hole / e Å^{-3}	1.73/-0.97
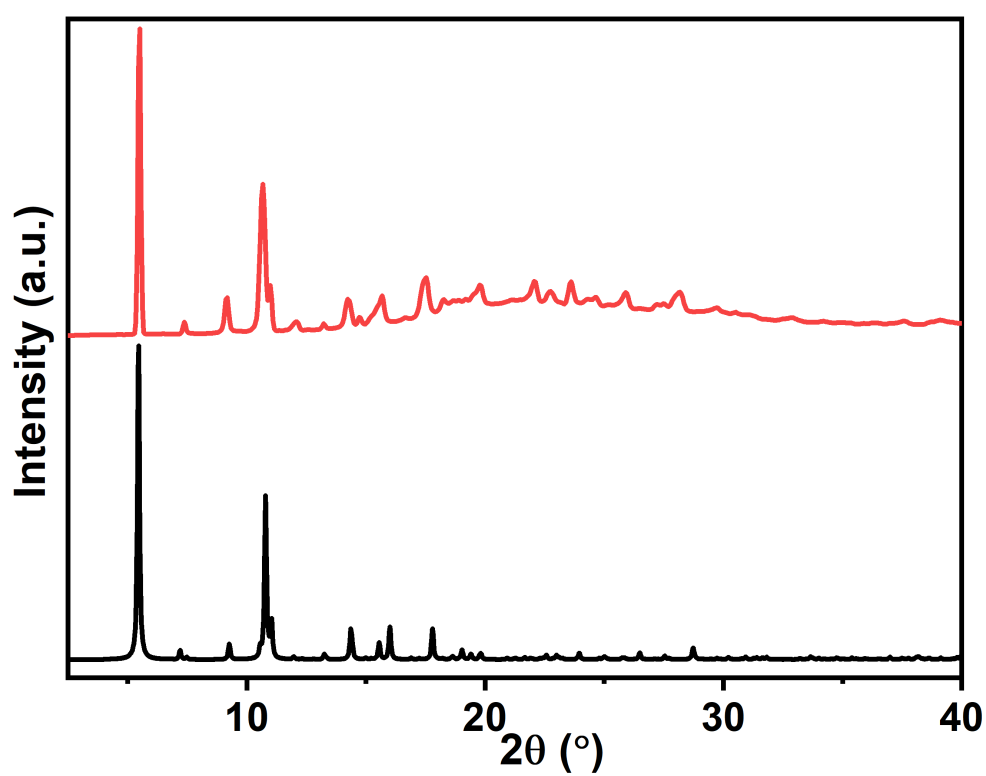
Figure S11. PXRD pattern of calculated $Cu_2(PTMTB)(H_2O)_2$ (black) and pristine $Cu_2(PTMTB)(H_2O)_2$ (red).
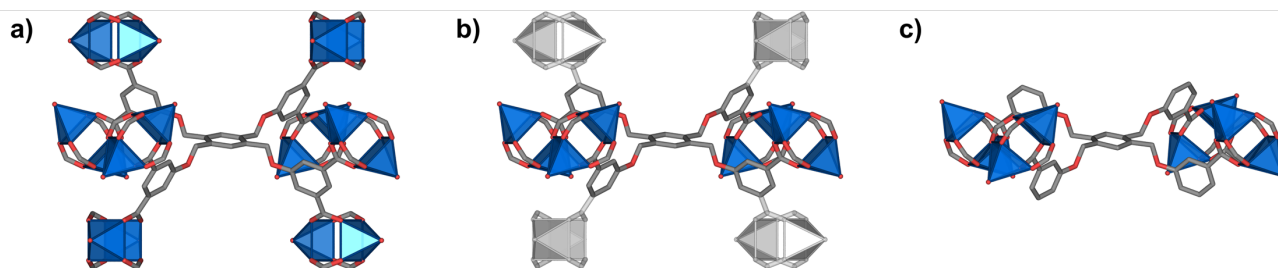
S3.4. Structural details

Figure S12. Highlight of a) the conformation of the PTMTI ligand in the crystal structure of Cu-**tbo**-MOF-**1**; b) the predicted conformation of the clipped ligand in a square conformation; and c) the conformation of PTMTB in $Cu_2(PTMTB)(H_2O)_2$ matching with the predicted by net-clipping. Note that the approach not only successfully predicted the topology of the MOF assembled with a new low-symmetry linker but also accurately anticipated the conformation adopted by the linker within the structure.
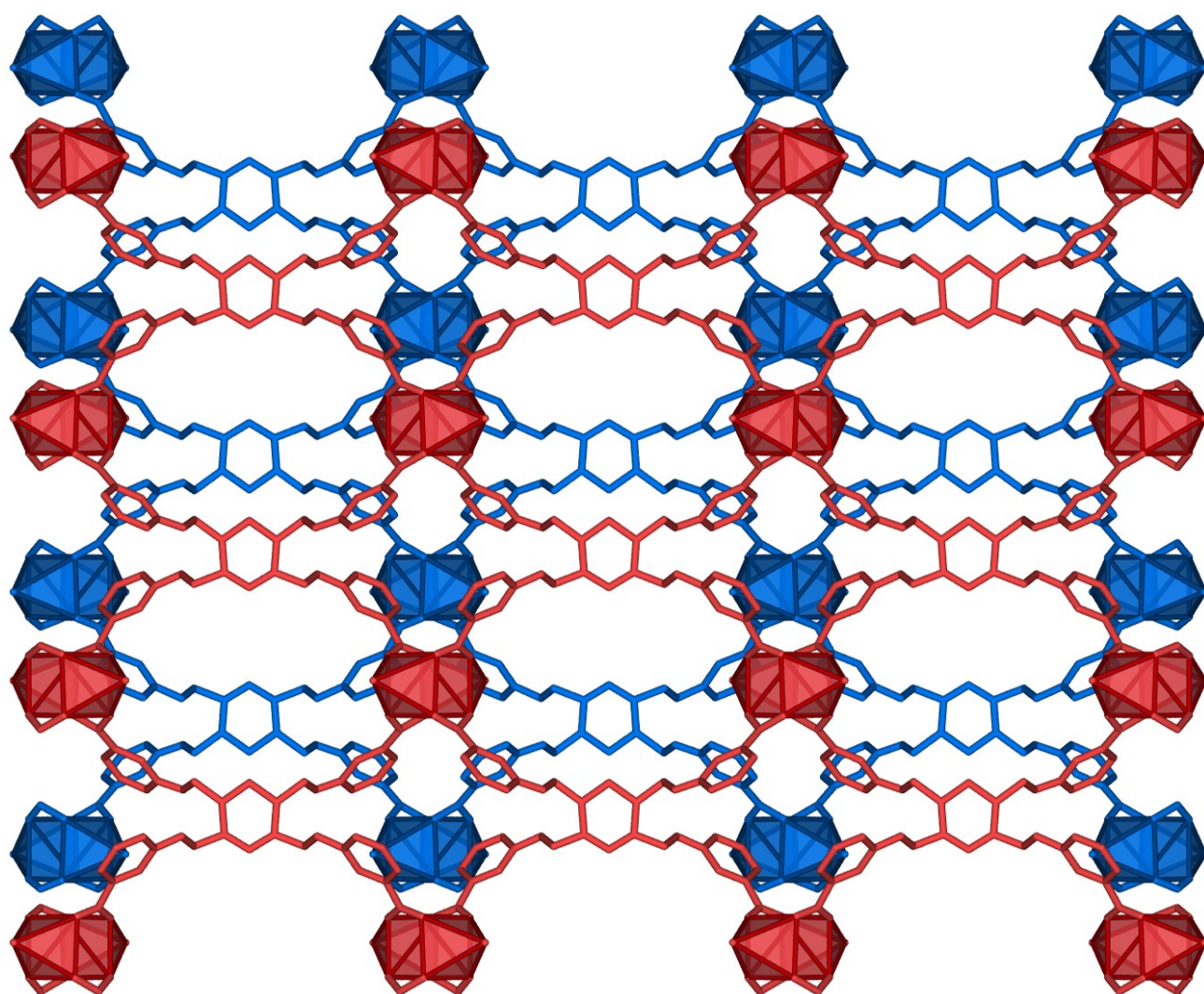
Figure S13. AB packing of the 2D $Cu_2(PTMTB)(H_2O)_2$ structure.

S4. Cu$_2$(TMBPTC)(H$_2$O)$_2$

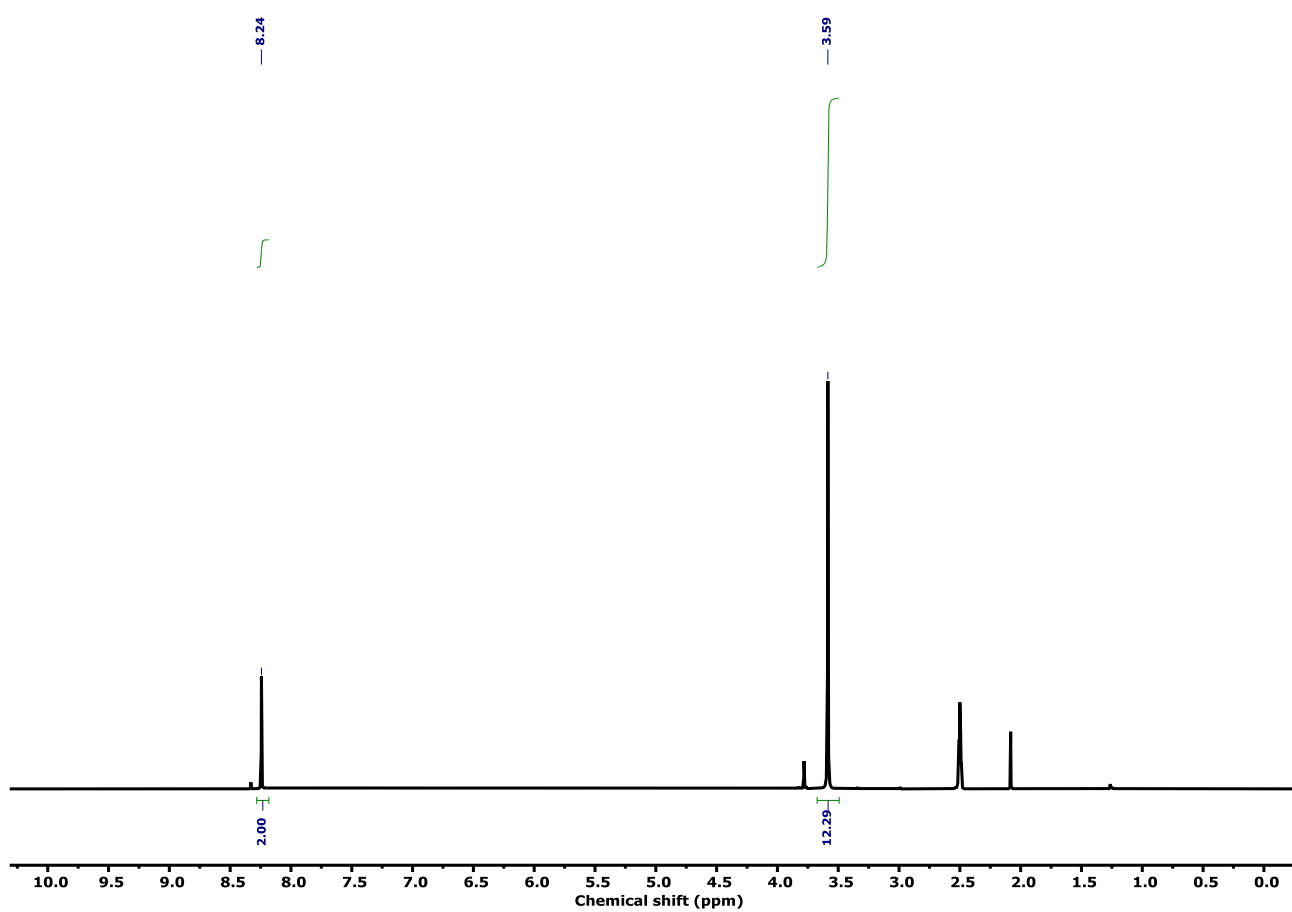## S4.1. ^{1}H and ^{13}C Nuclear Magnetic Resonance

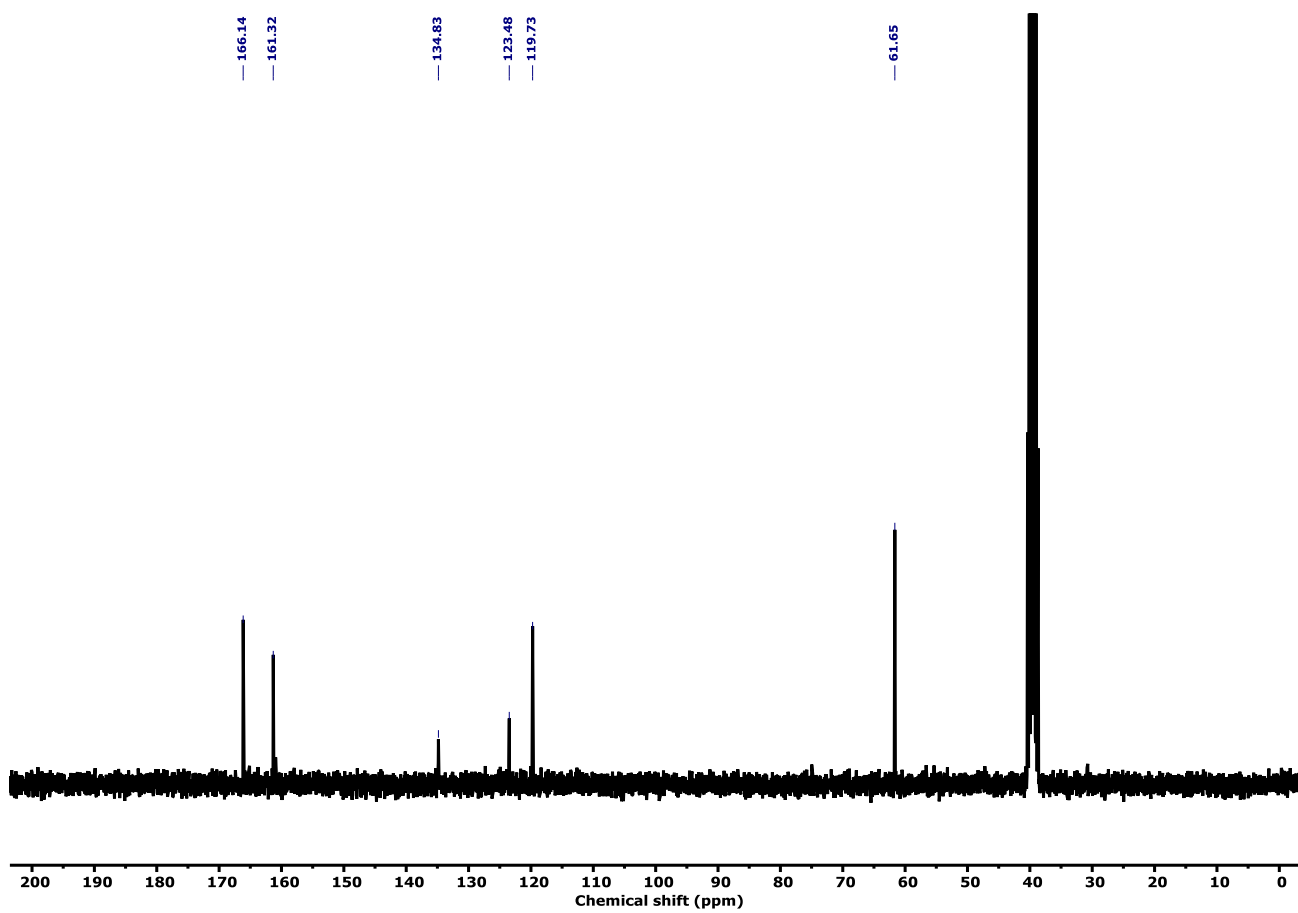**Figure S14.** ^{1}H NMR spectrum (300 MHz, DMSO-d_6) of H$_4$TMBPTC.

Figure S15. ^{13}C NMR spectrum (75 MHz, DMSO-d_6) of H$_4$TMBPTC.

S4.2. Single-crystal X-ray diffraction

Table S3. Crystal data and structure refinement for Cu$_2$(TMBPTC)(H$_2$O)$_2$

Identification code	CCDC-2270218
Empirical formula	C$_{26}$H$_{28}$Cu$_2$N$_2$O$_{14}$
Formula weight	719.58
Temperature/K	100
Crystal system	monoclinic
Space group	C2/c
a/Å	34.7885(7)
b/Å	11.2616(2)
c/Å	20.4116(4)
α/°	90
β/°	123.683(2)
γ/°	90
Volume/Å^3	6654.2(3)
Z	8
ρ$_{calc}$g/cm^3	1.437
μ/mm^{-1}	2.020
F(000)	2944.0
Crystal size/mm^3	0.08 × 0.08 × 0.07
Radiation	synchrotron (λ = 0.82656)
2Θ range for data collection/°	3.272 to 52.778
Index ranges	-35 ≤ h ≤ 31, 0 ≤ k ≤ 12, 0 ≤ l ≤ 21
Reflections collected	25884
Independent reflections	4166 [R$_{int}$ = 0.2282, R$_{sigma}$ = 0.1471]
Data/restraints/parameters	4166/134/381
Goodness-of-fit on F^2	1.083
Final R indexes [I>=2σ (I)]	R$_1$ = 0.0797, wR$_2$ = 0.2317
Final R indexes [all data]	R$_1$ = 0.1005, wR$_2$ = 0.2420
Largest diff. peak/hole / e Å^{-3}	2.11/-0.73
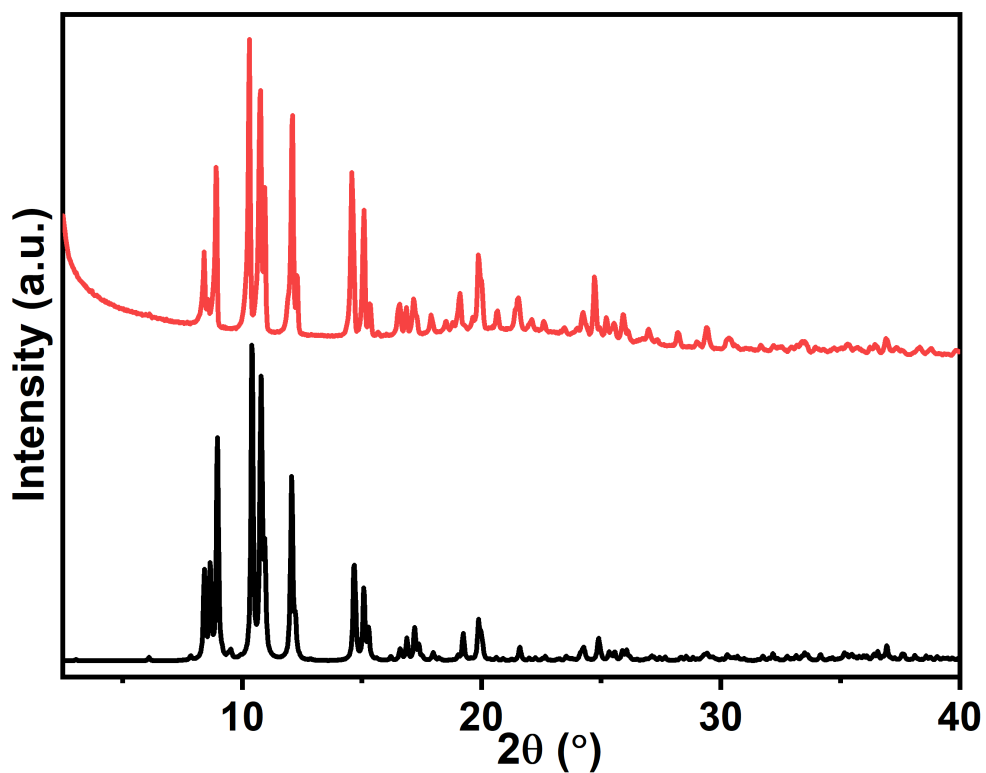
Figure S16. PXRD pattern of calculated $Cu_2(TMBPTC)(H_2O)_2$ (black) and pristine $Cu_2(TMBPTC)(H_2O)_2$ (red).
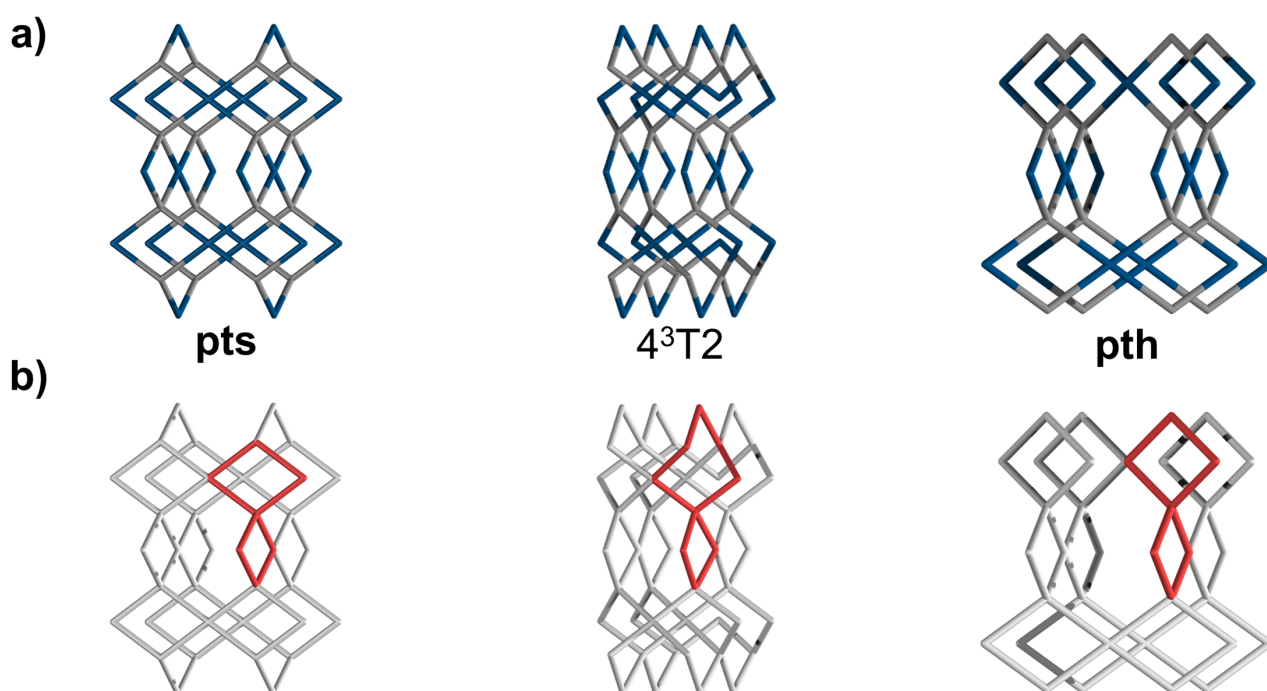
Figure S17. a) Net representation of the **pts** (left), 4^3T2 (centre) and **pth** (right) topologies, in blue the square node and gray tetrahedral node. b) Highlight of some characteristic circuits of connections in **pts** (left), 4^3T2 (centre) and **pth** (right) topologies, comparing 2 adjacent 4-cycles which are in 90º or 45º respect each other in **pts** or **pth**, respectively; while in the new 4^3T2 net there is a 6-cycle adjacent to the 4-cycle due to the desymmetrization of the square nodes in two positions, inducing a shift in the position of the tetrahedral nodes.
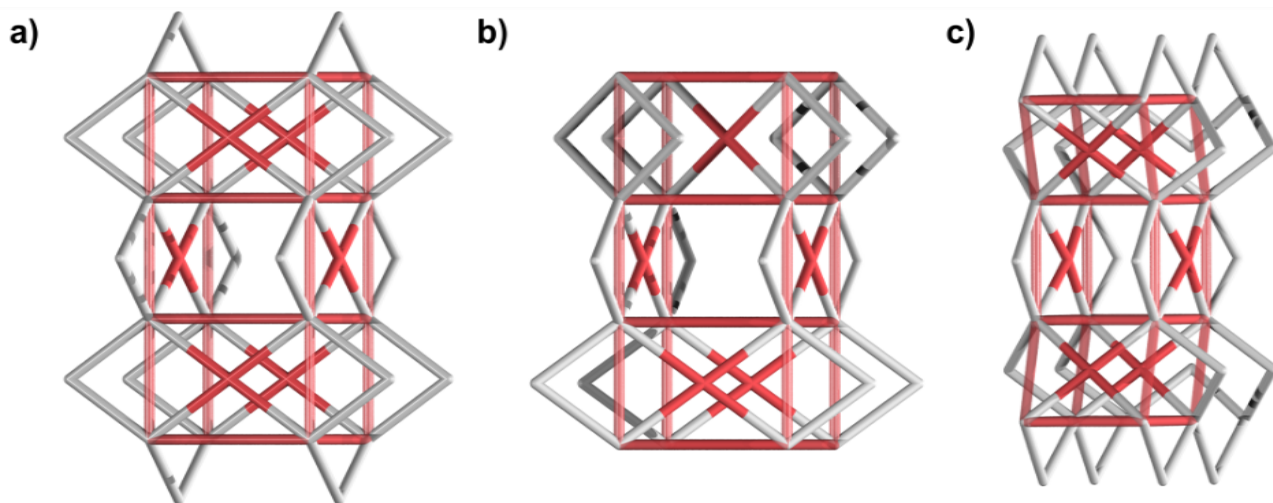
Figure S18. Highlight of the tetrahedral MBBs arrangement in a primitive cubic conformation in the a) **pts** net, b) **pth** net and c) 4^3T2 net. Note here that the tetrahedral nodes are in the same position in **pts** and **pth** topologies, while in the 4^3T2 net there is a shift between two contiguous cubes. The square nodes, highlighted in red, are a) alternated in the faces of the cubes in different axis in the **pts** net; b) alternated in the same way as in **pts** net with an additional square connecting tetrahedral nodes in the diagonal of the cube in the **pth** net; and c) alternated in the faces of the cubes in different axis with a slight inclination in the 4^3T2 net respect to the **pts** net.

S5. Cu(TMBPDC)(H₂O)
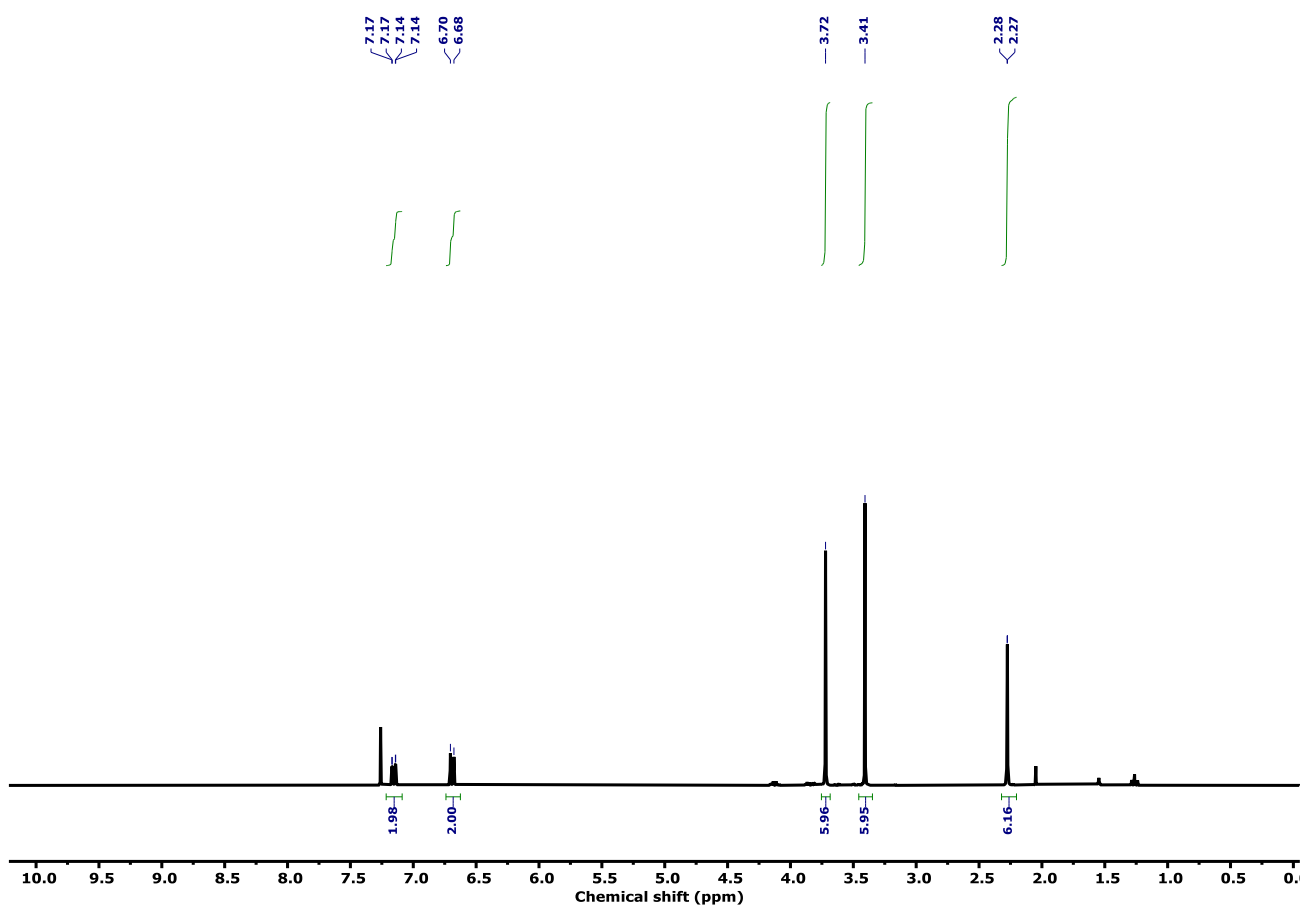
S5.1. ¹H and ¹³C Nuclear Magnetic Resonance

Figure S19. ¹H NMR spectrum (300 MHz, CDCl₃) of 2,2',6,6'-tetramethoxy-3,3'-dimethyl-1,1'-biphenyl.
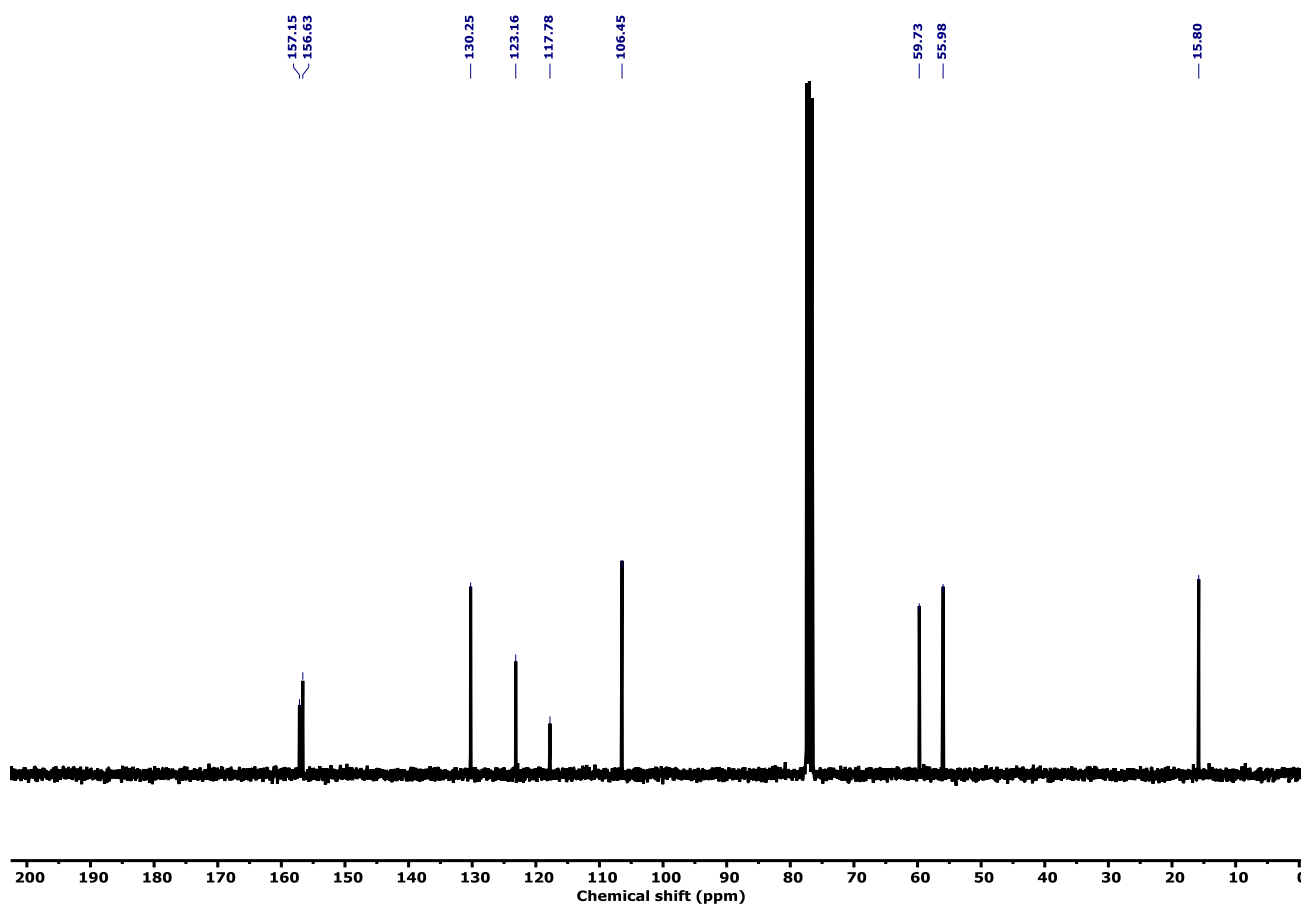
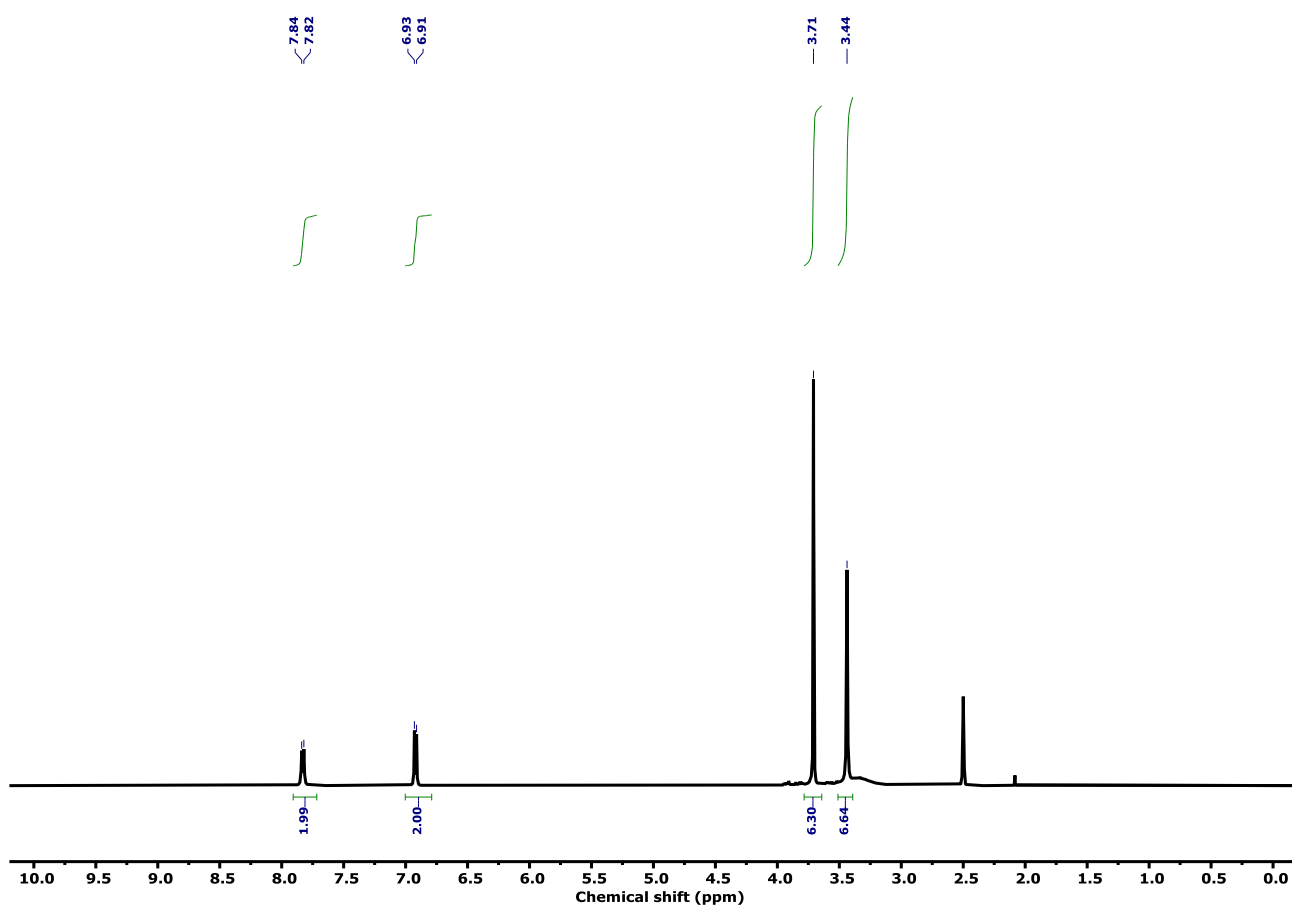**Figure S20.** ^{13}C NMR spectrum (75 MHz, CDCl$_3$) of 2,2',6,6'-tetramethoxy-3,3'-dimethyl-1,1'-biphenyl.

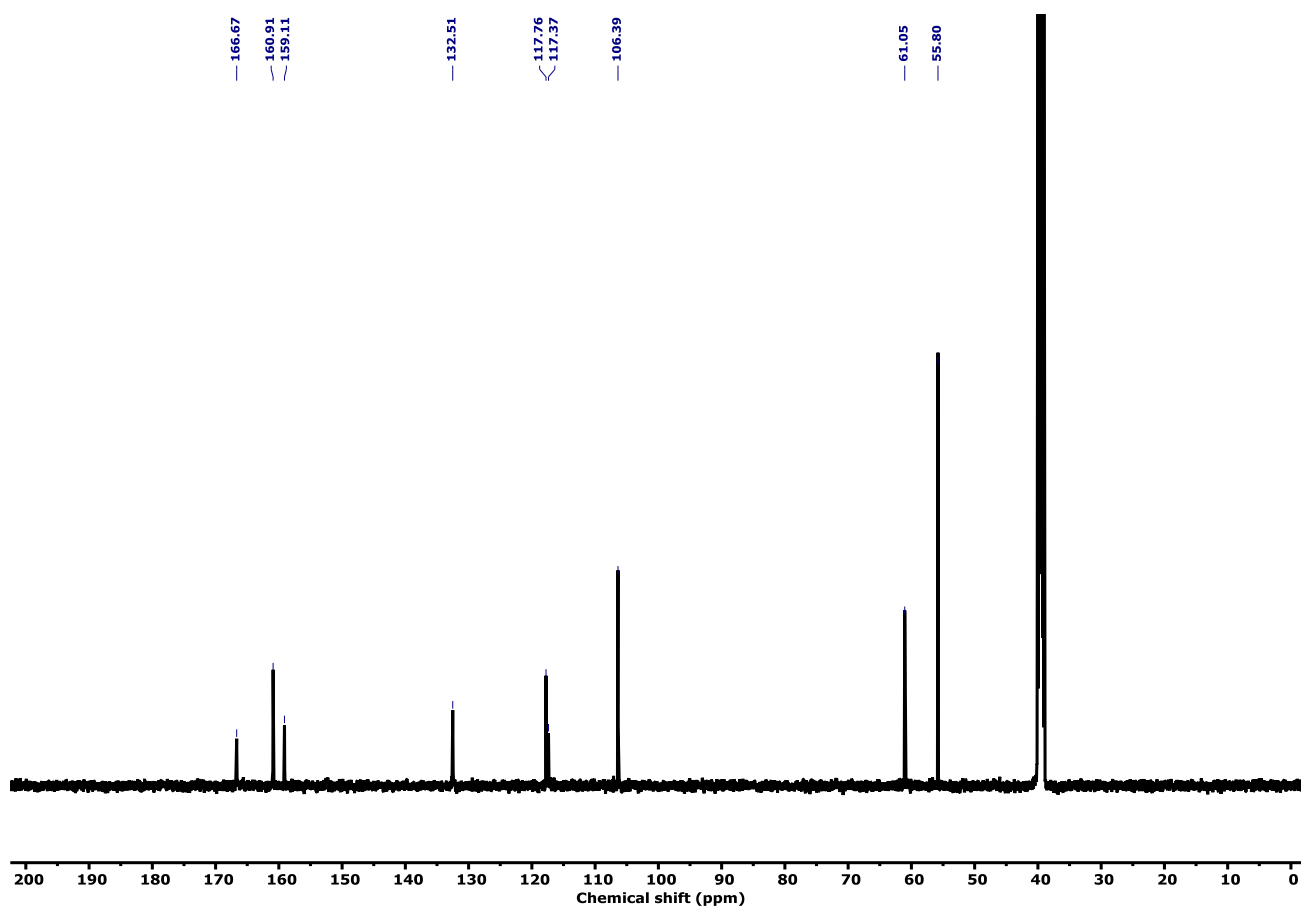**Figure S21.** ^{1}H NMR spectrum (500 MHz, DMSO-d_6) of H$_2$TMBPDC.

Figure S22. ^{13}C NMR spectrum (125 MHz, DMSO-d_6) of H$_2$TMBPDC.

S5.2. Single-crystal X-ray diffraction

Table S4. Crystal data and structure refinement for Cu(TMBPDC)(H$_2$O)

Identification code	CCDC-2270220
Empirical formula	C$_{21}$H$_{23}$CuNO$_9$
Formula weight	496.94
Temperature/K	100
Crystal system	monoclinic
Space group	P2$_1$/c
a/Å	11.306(4)
b/Å	14.8702(3)
c/Å	13.0779(4)
α/°	90
β/°	108.499(2)
γ/°	90
Volume/Å^3	2085.1(7)
Z	1
ρ$_{calc}$g/cm^3	1.583
μ/mm^{-1}	1.655
F(000)	1028.0
Crystal size/mm^3	0.09 × 0.08 × 0.06
Radiation	synchrotron (λ = 0.82656)
2Θ range for data collection/°	4.418 to 67.888
Index ranges	-12 ≤ h ≤ 11, -18 ≤ k ≤ 0, -17 ≤ l ≤ 16
Reflections collected	26209
Independent reflections	4377 [R$_{int}$ = 0.1020, R$_{sigma}$ = 0.0947]
Data/restraints/parameters	4377/0/295
Goodness-of-fit on F^2	1.094
Final R indexes [I>=2σ (I)]	R$_1$ = 0.0484, wR$_2$ = 0.1433
Final R indexes [all data]	R$_1$ = 0.0555, wR$_2$ = 0.1484
Largest diff. peak/hole / e Å^{-3}	0.64/-1.44

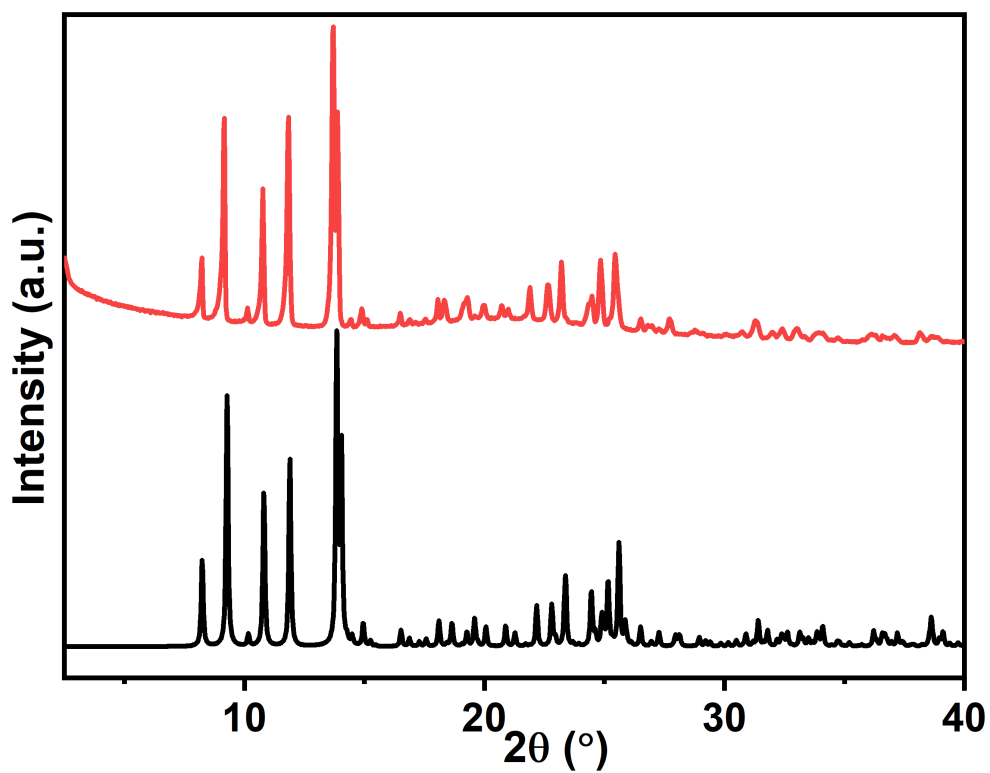**Figure S23.** PXRD pattern of calculated Cu(TMBPDC)(H₂O) (black) and pristine Cu(TMBPDC)(H₂O) (red).
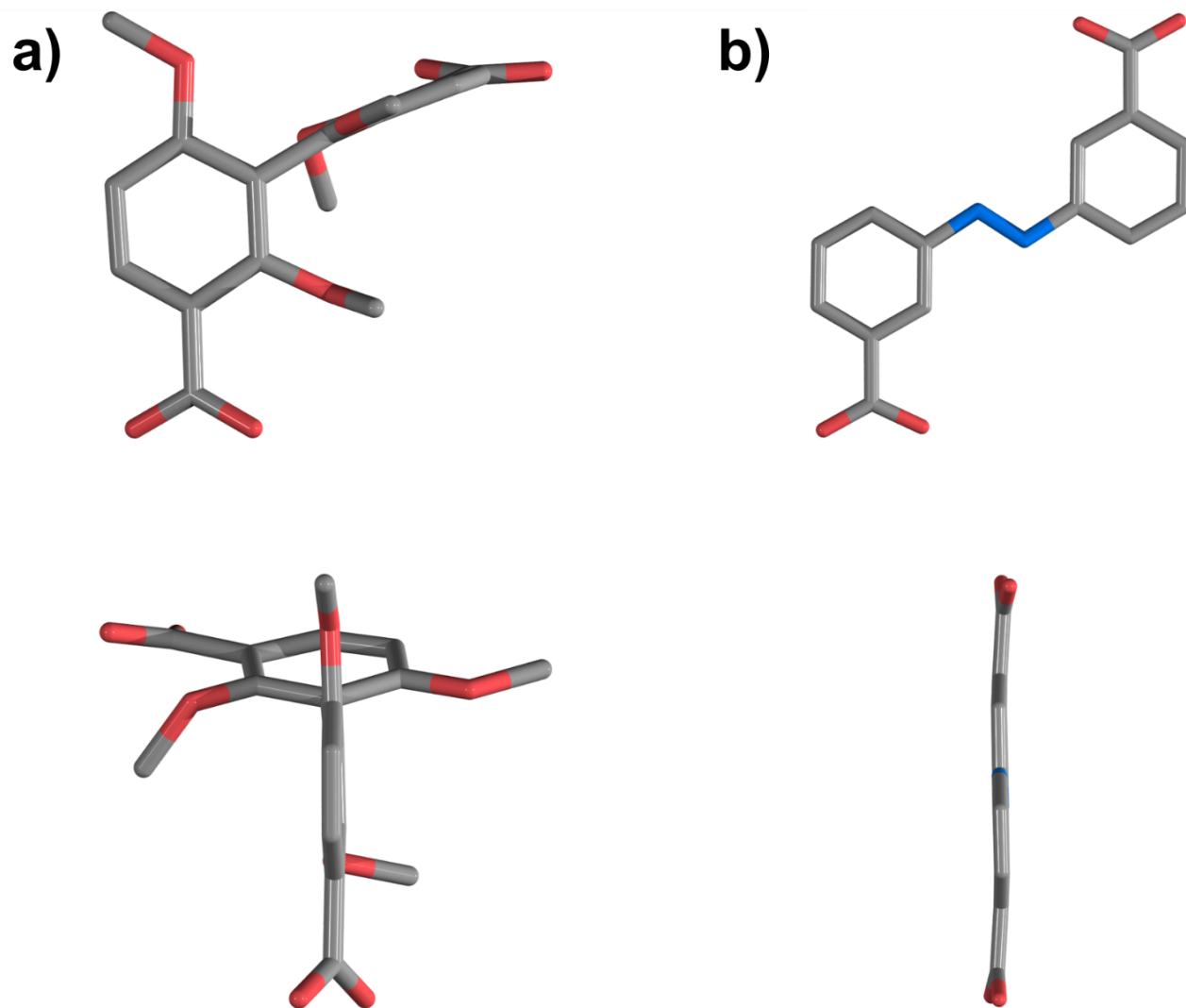
Figure S24. a) TMBPDC and b) ABDC linkers showing the difference on the directionality of the carboxylates in the T-T and zigzag conformations, producing the reticulation of different structures when combining with Cu(II)-paddlewheels in a 1D metal-organic chain or in a 2D metal-organic layer, respectively.

S6. Net-clipping of COFs

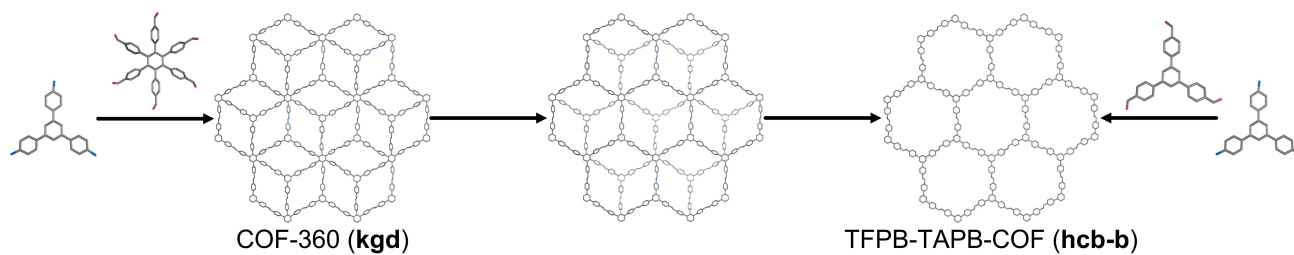COF-360 (**kgd**)   TFPB-TAPB-COF (**hcb-b**)

Figure S25. Schematic of the net-clipping approach applied to the formation of reticular materials hexagonal HFPB ligand to trigonal TFPB combined with 3-c triaminephenilbenzene MBBs.

S7. References

1   H. Wondratschek and U. Müller, *International Tables for Crystallography, Volume A1: Symmetry relations between space groups*, Springer, Dordrecht, 2004.
2   Z. Chen, Z. Thiam, A. Shkurenko, L. J. Weselinski, K. Adil, H. Jiang, D. Alezi, A. H. Assen, M. O'Keeffe and M. Eddaoudi, *J. Am. Chem. Soc.*, 2019, **141**, 20480–20489.
3   Z. Zhang, C. Chen, Q. Wang, Z. Han, X.-Q. Dong and X. Zhang, *RSC Adv.*, 2016, **6**, 14559-14562.
4   J. Juanhuix, F. Gil-Ortiz, G. Cuní, C. Colldelram, J. Nicolás, J. Lidón, E. Boter, C. Ruget, S. Ferrer and J. Benach, *J. Synchrotron Radiat.*, 2014, **21**, 679–689.
5   W. Kabsch, *Acta Cryst. D*, 2010, **66**, 133–144.
6   G. M. Sheldrick and IUCr, *Acta Cryst. A*, 2015, **71**, 3–8.
7   G. M. Sheldrick and IUCr, *Acta Cryst. C*, 2015, **71**, 3–8.
8   O. V. Dolomanov, L. J. Bourhis, R. J. Gildea, J. A. K. Howard and H. Puschmann, *J. Appl. Cryst.*, 2009, **42**, 339–341.